
TEMPORAL SIMILARITY METRICS FOR LATENT NETWORK RECONSTRUCTION: THE ROLE OF TIME-LAG DECAY

A PREPRINT

Hao Liao

National Engineering Laboratory for Big Data System Computing Technology
Guangdong Province Key Laboratory of Popular High Performance Computers
College of Computer Science and Software Engineering
Shenzhen University
Shenzhen 518060, PR China

Ming-Kai Liu

National Engineering Laboratory for Big Data System Computing Technology
Guangdong Province Key Laboratory of Popular High Performance Computers
College of Computer Science and Software Engineering
Shenzhen University
Shenzhen 518060, PR China

Manuel Sebastian Mariani

Institute of Fundamental and Frontier Sciences
University of Electronic Science and Technology of China
Chengdu 610051, PR China
URPP Social Networks
Universität Zürich
CH-8050 Switzerland

Mingyang Zhou

National Engineering Laboratory for Big Data System Computing Technology
Guangdong Province Key Laboratory of Popular High Performance Computers
College of Computer Science and Software Engineering
Shenzhen University
Shenzhen 518060, PR China

Xingtong Wu

National Engineering Laboratory for Big Data System Computing Technology
Guangdong Province Key Laboratory of Popular High Performance Computers
College of Computer Science and Software Engineering
Shenzhen University
Shenzhen 518060, PR China

April 5, 2019

ABSTRACT

When investigating the spreading of a piece of information or the diffusion of an innovation, we often lack information on the underlying propagation network. Reconstructing the hidden propagation paths based on the observed diffusion process is a challenging problem which has recently attracted attention from diverse research fields. To address this reconstruction problem, based on static simi-

ilarity metrics commonly used in the link prediction literature, we introduce new node-node temporal similarity metrics. The new metrics take as input the time-series of multiple independent spreading processes, based on the hypothesis that two nodes are more likely to be connected if they were often infected at similar points in time. This hypothesis is implemented by introducing a time-lag function which penalizes distant infection times. We find that the choice of this time-lag strongly affects the metrics' reconstruction accuracy, depending on the network's clustering coefficient and we provide an extensive comparative analysis of static and temporal similarity metrics for network reconstruction. Our findings shed new light on the notion of similarity between pairs of nodes in complex networks.

Keywords Information networks · Network reconstruction · Temporal similarity · Innovation diffusion

1 Introduction

Our understanding of social networks is affected by the fact that, typically, we only have incomplete knowledge about the topology of real networks [16, 5]. Aimed at overcoming this shortcoming, the problem of reconstructing missing links has attracted enormous attention from scholars from diverse fields (see [53] for a recent review on the problem). Existing approaches to the network reconstruction problem include the use of local structural metrics [43, 53, 19], global walk-counting methods [39, 53], stochastic block models [33], fitness-based methods [14], structural perturbation analysis [50, 47], machine-learning techniques [31], among many others. Scholars have aimed to identify missing connections in a wide variety of systems, including protein-protein interaction networks [41], neural networks [10], citation networks [15], and social networks [49, 4].

In parallel, there has been recent interest [59, 63, 28, 83, 68, 48] on a different problem of network reconstruction: if we are only provided with information on the outcome of a dynamical process on an unknown propagation network, can we reconstruct the propagation network? The problem – which has been referred to as *latent network reconstruction* [59] – can be included in the broader class of problems that aim to reconstruct the properties of a spreading process (for instance, the seed node [9] or the epidemic parameters [59]) from data on observed realizations of the process. The question is fundamentally different from the traditional link prediction problem [53]: while link prediction studies [53] typically assume that only part of the network is hidden and needs to be reconstructed, here we assume that the topology of the propagation network is completely hidden. The reconstruction problem studied here is important as we often deal with datasets where the propagation network is largely unknown: for instance, the owners of an online e-commerce platform might have complete information on the time-series of users' purchases, but lack information about the social connections between the users which might have affected, to some extent, the observed purchasing patterns.

Existing works have tackled the latent network reconstruction problem from various perspectives. Among the most relevant contributions, Myers et al. [59] addressed the problem through a maximum-likelihood estimation method based on a cascade spreading model, which was further mapped into a convex optimization problem. Gomez-Rodriguez et al. [28] developed a faster maximum-likelihood method based on a cascade propagation model. Shen et al. [68] leveraged compressed sensing theory to map the network reconstruction problem into a convex optimization problem. Such a mapping is non-trivial and model-specific; they solved the problem for the Susceptible-Infected-Susceptible (SIS) and the "contact process" dynamics [68]. The main limitation of these approaches is that they are model-dependent: Different spreading models require the solution of a different set of equations. For example, in the compressed-sensing theory approach, the convex-optimization equations for the SIS and the contact process model differ substantially [68]. Besides, the compressed-sensing approach to network reconstruction can be only applied to sparse networks [68].

On the other hand, other studies [83, 48] have tackled the latent network reconstruction problem by means of simple similarity metrics. With respect to convex optimization [59] and methods based on compressed sensing theory [68], similarity metrics have two main advantages: (1) They do not depend on the specific spreading model considered; (2) Their implementation is faster. Temporal similarity metrics for the latent network reconstruction [48] build on the hypothesis that two nodes are more likely to be connected if independent spreading processes tend to infect them at similar times. A simple way to implement this assumption is to impose, for each pair (i, j) of nodes that are infected by the same spreading process, a contribution to their similarity s_{ij} in the form of a power-law decreasing function of the time lag between the two infection times [48]. For this reason, we refer to these metrics as temporal similarities with *power-law time lag decay*.

Here, we develop new temporal similarity indexes based on the hypothesis that two nodes are more likely to be connected if independent spreading processes tend to infect them at two consecutive time steps of the dynamics. We refer to the new metrics as temporal similarities with *one-step time lag decay*. Based on the power-law and one-step decay functions, for each of the eight classes of structural similarity metrics considered here, we construct two corresponding

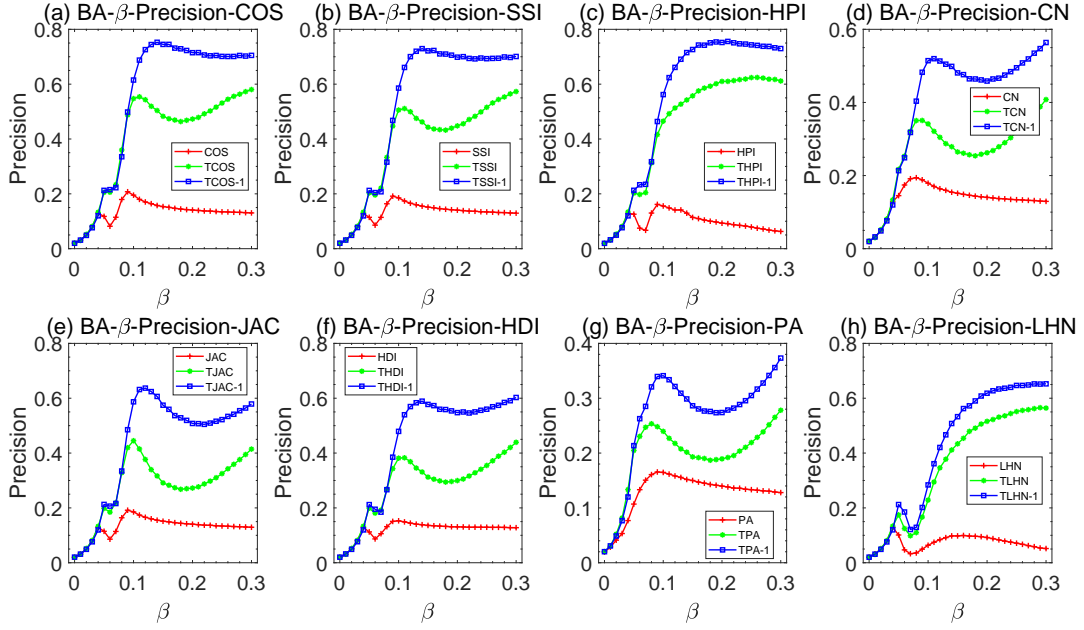


Figure 1: Reconstruction precision of different similarity metrics as a function of β for eight classes of similarity metrics (CN, COS, SSI, HPI, JAC, HDI, PA, LHN), for the SIR dynamics ($f = 0.5$) on BA networks ($N = 500$, $\langle k \rangle = 5$). The results are averaged over 50 independent realizations. For sufficiently large β values, temporal similarity metrics with one-step time-lag decay substantially outperform temporal similarity metrics with power-law time-lag and static metrics.

temporal similarity metrics. We compare their performance in reconstructing the whole propagation network in both synthetic and real data. By analyzing 40 empirical networks, we provide the first systematic performance comparison of temporal similarity metrics based on different classes of structural similarity metrics.

We find that for the Susceptible-Infected-Recovered (SIR) spreading dynamics [64], for almost all the analyzed networks, the temporal similarities with one-step time lag decay outperform the temporal similarities with a power-law time lag decay. The performance gap is substantially larger for spreading processes sufficiently above their critical point. Besides, among all the classes of similarity metrics considered, we find that the temporal similarity metric with one-step time-lag decay based on the Cosine similarity [67] tends to outperform the other metrics; other competitive classes of similarity are the temporal variants of the Sorensen index [69] and the Jaccard similarity [37]. Results for two additional spreading models (Susceptible-Infected, SI, and Linear Threshold Model, LTM) are in qualitative agreement.

Our findings move the first steps toward an extensive benchmarking of methods for the reconstruction of a hidden topology from the available event time-series of a spreading process. Our work sheds new light on the notion of node-similarity based on the outcome of dynamical processes on networks, and it has potential implications for social network analysis that will be outlined in the Discussion section.

2 Results

2.1 Problem statement

We assume that there is a unipartite network (whose adjacency matrix is denoted by A) whose topology is unknown, and our goal is to reconstruct it. Our available information is the time-stamped list of adoptions of multiple items that diffuse through a given spreading process. Entry $(i, \alpha, t_{i\alpha})$ in this list tells us that node i adopted item α at time $t_{i\alpha}$. The adoption processes considered here is ruled by the SIR dynamics [64]: the "adoption" of item α corresponds to the "infection" during realization α of the SIR dynamics. For this reason, in the following, we will use "adoption" and "infection" interchangeably.

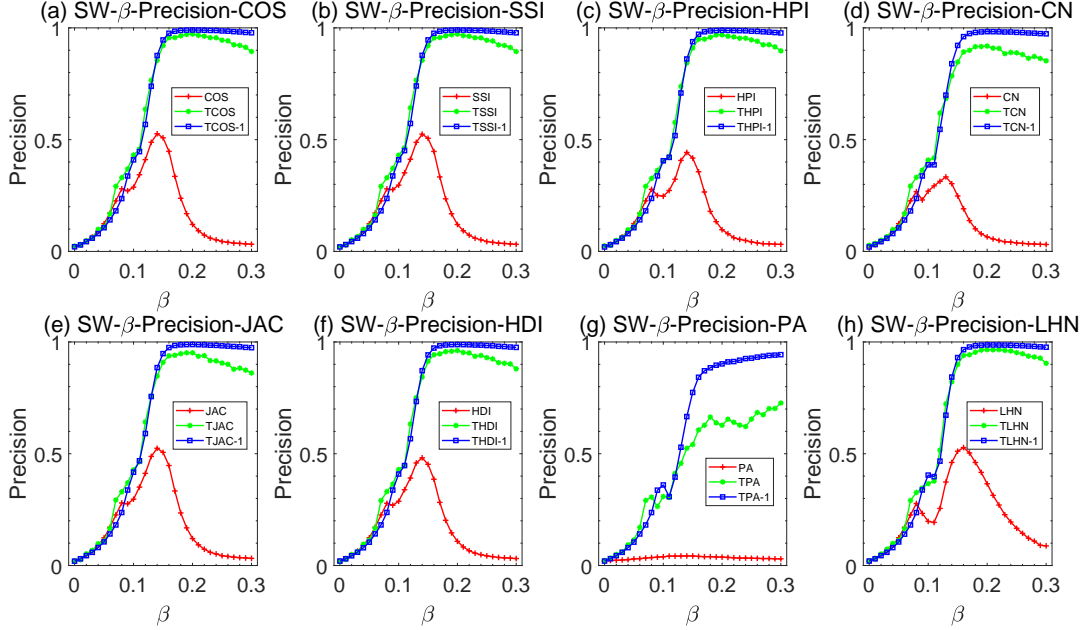


Figure 2: (Color online) Reconstruction precision of different similarity metrics as a function of β for eight classes of similarity metrics (CN, COS, SSI, HPI, JAC, HDI, PA, LHN), for the SIR dynamics ($f = 0.5$) on SW networks ($N = 500$, $P = 0.1$, $\langle k \rangle = 5$). The results are averaged over 50 independent realizations. For sufficiently large β values, temporal similarity metrics with one-step time-lag decay substantially outperform temporal similarity metrics with power-law time-lag and static metrics.

We consider 40 empirical unipartite networks; among these, 20 are information networks (details in the Supplementary Material). We generate the time-series $\{(i, \alpha, t_{i\alpha})\}$ of adoptions by running, for each network, 50 independent realizations of the SIR spreading dynamics initiated by a fraction f of initiators (see Methods for details) [48]. Each independent realization α of the spreading process is therefore interpreted as an item that gradually diffuses across the network. In fact, the time-series $\{(i, \alpha, t_{i\alpha})\}$ can be interpreted as a temporal bipartite network [34]; we denote by R the incidence matrix of the corresponding time-aggregate bipartite network: $R_{i\alpha} = 1$ if node i adopted item α .

We address the following problem. Assuming that we only know $\{(i, \alpha, t_{i\alpha})\}$, which is the best method to reconstruct the E edges of A from $\{(i, \alpha, t_{i\alpha})\}$? While, in principle, several techniques of network reconstruction can be designed [53, 68, 48], we narrow our focus to similarity metrics that aim to infer the similarity s_{ij} of two nodes i and j based on their co-adoption patterns [83, 48]. The definitions of the metrics of interest are provided in Sections 2.2 and 4.1.

Such similarity metrics produce a ranking of the pairs of nodes (potential edges) in descending order of s_{ij} . Assuming that we know the number of edges E of the underlying propagation network A , the E top-ranked links by s_{ij} form the network $A^{(s)}$ reconstructed by metric s . It is natural to assess the precision of the metric s_{ij} by measuring the fraction of common links between A and $A^{(s)}$. This metric is typically referred to as precision in the link prediction [53] and information filtering literature, and we use it to evaluate the reconstruction performance of the similarity metrics. The results for another evaluation metric¹ (Area Under the Curve, AUC [51]) are in qualitative agreement with those obtained with the precision (Figs. S8).

2.2 From structural to temporal similarity metrics

We consider here eight classes of structural similarities [53]: common neighbors (CN), Jaccard Index (Jac), Leicht-Holme-Newman Index (LHN), Cosine Index (COS), Sorensen Index (SSI), Hub Promoted Index (HPI), Hub Depressed Index (HDI), Preferential Attachment (PA). These structural metrics have been used by researchers from diverse domains to address various problems in network analysis. They have been applied to the reconstruction of missing links in networks where only a part of the topology is available [16, 51], to the prediction of new connections in social and information systems [49], and to the latent network reconstruction problem studied here as well [83].

¹Differently from the precision metric, the AUC metric is independent of E .

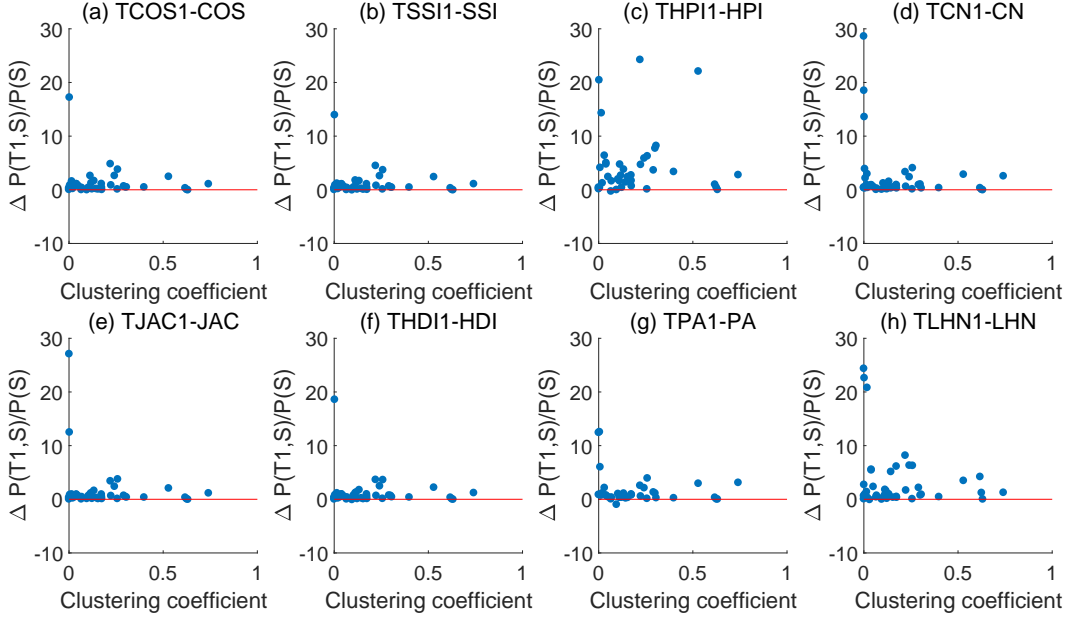


Figure 3: Reconstruction precision relative difference $\Delta P(T1, S)/P(S) = (P(T1) - P(S))/P(S)$ as a function of the network clustering coefficient. Each dot represents an empirical network; we analyzed 40 empirical contact networks. For all classes of similarity, almost all the empirical networks fall above the $P(T1) = P(S)$ red line. We use $\beta = 4\beta_c$ and $f = 0.5$ here. The results are averaged over 50 independent realizations.

For each class² X of similarities, we consider the standard static metric [53] (directly denoted as X), and two *temporal* similarity metrics: temporal metrics with the power-law time-lag decay (denoted as TX) [48], and the new temporal metrics with the one-step time-lag decay (denoted as $TX1$). The last two classes of metrics differ in how the similarity score of a given pair (i, j) of nodes depends on the *time lag* $t_{i\alpha} - t_{j\alpha}$ between node i 's and j 's adoption times $t_{i\alpha}$ and $t_{j\alpha}$ for item α . We refer to the Methods section for all the definitions.

To illustrate the main idea behind each class of metrics, we define here the common-neighbors metrics: static common neighbors (CN), temporal common neighbors with a power-law decay of time-lag (TCN), and temporal common neighbors with one-step decay of time lag (TCN1). The common neighbors (CN) of a given pair (i, j) of nodes is simply given by [53]

$$s_{ij}^{CN} = \sum_{\alpha} R_{i\alpha} R_{j\alpha}. \quad (1)$$

According to this definition, two nodes are similar (and, therefore, more likely to be connected in the hidden unipartite network) if they often adopted the same item.

Zeng [83] found that this metric and similar *static* metrics can be used to reconstruct the topology of a hidden network based on the time-series of a spreading dynamics. Subsequently, the static metric proved to be sub-optimal with respect to time-aware metrics [48]. Indeed, while it is plausible that two nodes that often adopt the same item at similar times are more likely to be connected, the same is not necessarily true if the common adoptions happen at very distant points in time: given two adopters i and j , with $t_{i\alpha} \ll t_{j\alpha}$, item α might indeed have reached j through a long network path, without the two nodes being directly connected.

To penalize longer time lags, [48] introduced the *temporal common neighbors with power-law time-lag decay* (TCN) as

$$s_{ij}^{TCN} = \sum_{\alpha} R_{i\alpha} R_{j\alpha} |t_{i\alpha} - t_{j\alpha}|^{-1} (1 - \delta_{t_{i\alpha}, t_{j\alpha}}). \quad (2)$$

This time-aware metric significantly outperforms its static counterpart, s^{CN} , in the latent network reconstruction [48]. However, as a consequence of the power-law function, the similarity s^{TCN} of a given pair of nodes receives substantial non-zero contributions also when the two nodes adopt the same item at substantially different times.

² X is a placeholder here. E.g., X can represent common neighbors CN.

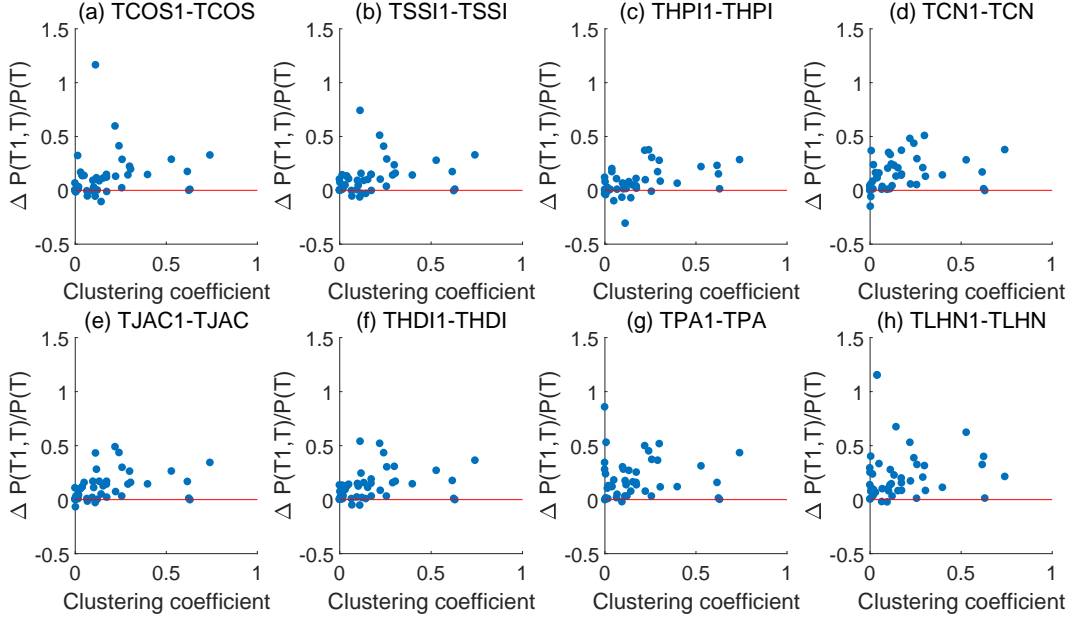


Figure 4: Reconstruction precision relative difference $\Delta P(T1, T)/P(T) = (P(T1) - P(T))/P(T)$ as a function of the network clustering coefficient. Each dot represents an empirical network; we analyzed 40 empirical contact networks. For all classes of similarity, almost all the empirical networks fall above the $P(T1) = P(T)$ red line; the only exceptions are some of the networks with low clustering coefficient. We use $\beta = 4\beta_c$ and $f = 0.5$ here. The results are averaged over 50 independent realizations.

In this work, we introduce the *temporal common neighbors with a one-step decay time-lag decay* (TCN1) as

$$s_{ij}^{TCN1} = \sum_{\alpha} R_{i\alpha} R_{j\alpha} \delta_{|t_{i\alpha} - t_{j\alpha}|, 1}. \quad (3)$$

According to this definition, the similarity s^{TCN1} of a given pair (i, j) of nodes only receives a contribution when the two nodes adopt the same item at two consecutive time steps.

Analogous definitions for the other seven classes of similarities and their temporal variants with power-law and one-step time-lag decay are provided in the Methods section. The goal of the rest of the paper is to extensively compare the performance of these metrics in reconstructing both synthetic and empirical networks.

2.3 Reconstruction of synthetic networks

We start our investigation from synthetic networks generated with the Barabási-Albert model [6] (see Methods for the generation details). Fig. 1 shows our reconstruction results: each panel refers to a class of similarities; for each class of similarities (e.g., common neighbors), we show the results for the static metric (CN), the temporal metric with power-law time lag decay (TCN), and the new temporal metric with one-step time lag decay (TCN1). The precision values attained by the metrics are shown as a function of the transmission probability β of the SIR spreading process.

For each considered structural metric (e.g., CN), for sufficiently large β values, the corresponding temporal metric with one-step decay (TCN1) performs significantly better than the corresponding temporal metric with power-law decay (e.g., TCN). As we reduce β , spreading processes tend to die out more rapidly, and it becomes increasingly harder to correctly reconstruct the underlying diffusion network; in the small- β regime, the temporal metrics with a one-step and power-law decay perform similarly. As expected [48], the time-aware metrics significantly outperform the static metric.

Fig. 2 shows analogous results for a small-world network [79] (see Methods for the generation details). We observe again a systematic performance edge of the temporal metrics with a one-step time lag decay over the temporal metrics with power-law time lag decay, yet this gap is smaller than in the BA networks.

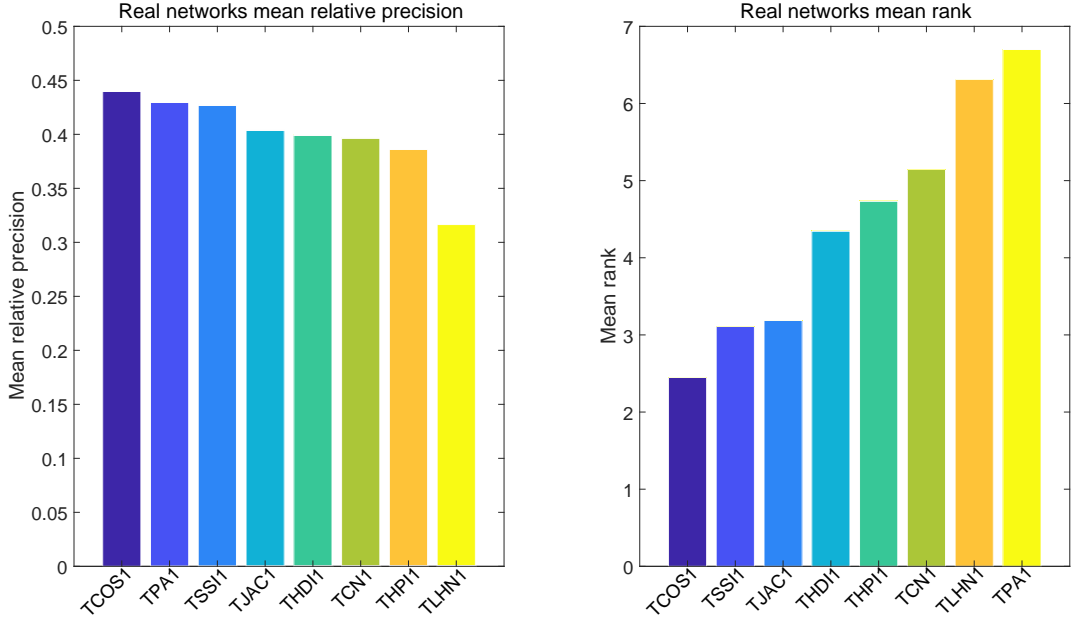


Figure 5: Mean relative precision (higher values correspond to better performance) and mean rank (lower values correspond to better performance) of the eight TX1 metrics. According to both evaluation metrics, TCOS1 is the best-performing metric, followed by TSS11 and TJAC1. We use $\beta = 4\beta_c$ and $f = 0.5$ here. The results are averaged over 50 independent realizations.

2.4 Reconstruction of real networks

Our results on synthetic networks suggest that the temporal metrics with one-step time lag decay reconstruct synthetic contact networks better than the temporal metrics with power-law time lag decay. To further validate this assertion, we analyzed 40 empirical contact networks of diverse nature including 20 information networks (details in the Supplementary Material).

For almost all the analyzed datasets, the temporal metrics with one-step time lag decay substantially improve the reconstruction accuracy with respect to both static (Fig. 3) and temporal metrics with power-law time lag decay (Fig. 4). The only networks where the temporal metrics with power-law time-lag decay can outperform the temporal metrics with one-step time-lag decay are those with low clustering coefficient³. This is intuitive: In a network with lower clustering, it is less likely that two non-connected nodes are reached by long propagation paths. This mitigates the advantage of considering only adoptions with one-step time lag when computing the similarity score of a given pair of nodes.

The results in Fig. 4 were obtained with $\beta = 4\beta_c$, where β_c is the epidemic threshold [64]. As expected from the synthetic network analysis, we find that for larger β values (Fig. S1), the one-step time lag metrics show better reconstruction accuracy for the vast majority of datasets and considered metrics. On the other hand, for lower β values, there is not a clear advantage of the metrics with the one-step time-lag decay (Figs. S2-S3).

So far, we have compared similarities of the same class (e.g., common neighbors) with different time-lag decay functions. A natural question arises: what is the relative performance of the eight temporal metrics TX1 with one-step time-lag decay obtained from the eight different classes of similarities? We compare the eight metrics' performance across the 40 empirical datasets considered here. We refer to Figs. S4-S5 for the results on individual datasets. To gain a general understanding of the metrics' performance, we aggregate the metrics' performance over the analyzed networks. To this end, we consider two evaluation metrics: the metrics' mean rank [58] and the mean relative precision.

³In our work, we use the average local clustering coefficient as a metric for clustering. For each node i in the network, we calculate the number K_i of existing edges that connect nodes that are connected with i , and the maximum number E_i of possible links between i 's neighbors. For an undirected graph, $E_i = k_i(k_i - 1)/2$. Finally, we define i 's local clustering coefficient $C_i = K_i/E_i$, and the network's clustering coefficient as $C = N^{-1} \sum_i C_i$.

To compute the metrics' mean rank, for each dataset d , we rank the eight TX1 metrics in order of decreasing precision. We denote by $r_d(s) \in \{1, 2, \dots, 8\}$ the ranking position metric s for dataset d . Given D analyzed empirical networks ($D = 40$ in our work), the mean rank $\overline{r(s)}$ of metric s is simply defined as $\overline{r(s)} = D^{-1} \sum_{d=1}^D r_d(s)$. Better performing metric should exhibit lower mean rank values [58]. In addition, denoting by $P_d(s)$ the precision achieved by metric s in dataset d , we define the mean relative precision $\overline{P(s)}$ of metric s as $D^{-1} \sum_{d=1}^D P_d(s) / \max_{s'} \{P_d(s')\}$. Better performing metric should exhibit larger mean relative precision values.

Both evaluation metrics lead to the same overall conclusion (Fig. 5): on average, the TCOS1 (temporal Cosine with one-step time-lag decay) metric

$$s_{ij}^{TCOS1} = \frac{\sum_{\alpha} R_{i\alpha} R_{j\alpha} \delta_{|t_{i\alpha} - t_{j\alpha}|, 1}}{\sqrt{\sum_{\alpha} R_{i\alpha} \sum_{\alpha} R_{j\alpha}}} \quad (4)$$

is the best-performing metric, followed by TSS1 and TJAC1 (see Methods for their definition). While TCOS1 provides us with a computationally fast metric to reconstruct the hidden topology, its mean precision is 0.349. This leaves the door open for future performance improvements, possibly based on new similarity metrics or more sophisticated methods.

3 Discussion

Our work provided a systematic benchmarking of temporal similarity metrics with respect to their accuracy in reconstructing a hidden network topology. The reconstruction was more accurate for SIR spreading processes with a large transmission probability, i.e., in the supercritical regime. On both real and synthetic networks, we found that temporal metrics with one-step time-lag decay perform systematically better than metrics with power-law time-lag decay. Besides, we found that the temporal cosine metric with one-step time-lag decay is the best-performing metric. Differently from maximum-likelihood methods [28] and compressed-sensing theory approaches [59], the temporal similarity metrics considered here are general and not restricted to a specific dynamics. In this sense, they can be interpreted not only as parsimonious and effective reconstruction tools, but also as general baselines against which more sophisticated, model-specific reconstruction techniques can be evaluated. While we focused on the SIR dynamics, we also assessed the metrics' performance for two additional spreading models: the Susceptible-Infected (SI) model [3, 70] and the Linear Threshold Model (LTM) [30, 40, 12]. The results obtained for these two models are in qualitative agreement with the results obtained for the SIR model (Figs. S6-S7), supporting the generality of our conclusions.

Our study paves the way for several extensions. Temporal similarity metrics might be applied to other network reconstruction problems, such as the problem where part of the topology is known [51] and the matching of user accounts across different domains or devices [11, 46]. Even more intriguingly, one can attempt to reconstruct the hidden topology of a social network based on the observed dynamics of real diffusion processes. For instance, from the observed spreading dynamics of many pieces of information, one might attempt to reconstruct propagation networks in social media [65] and e-commerce platforms [56]. The results presented here support metrics based on one-step time lags as the best-performing ones in the latent network reconstruction task. While the time step of the dynamics is unambiguously defined for simulated processes, the same does not hold for real spreading processes. Using temporal similarity metrics to reconstruct propagation topologies based on real time-series data will likely require us to first identify the typical timescale needed for a given piece of information to be transmitted from an individual to another, and then to use this typical timescale as the time-lag parameter in the similarity metric.

Finally, our work contributes to the rich literature on similarity on social and information networks [45, 44, 73, 29, 13, 66]. Previous research has stressed the role of structural similarity metrics, i.e., similarity metrics based either on the time-aggregate contact network of individuals (who is connected to whom) [35, 80, 42] or on the time-aggregate user-item bipartite adoption network (who collected what) [44, 83]. Here, we combined structure and temporal information (who collected what at which time) to define temporal similarity metrics that are effective in the propagation network task. We envision that future research on social and information network analysis might further develop simple yet well-performing time-aware metrics for network reconstruction.

4 Methods

4.1 Temporal similarity metrics

For each class C of similarity metrics, we define three metrics: a static metric C , a temporal metric with power-law time-lag decay TC , and a temporal metric with one-step time-lag decay $TC1$. In our work, we consider eight classes C of similarities: Common Neighbors (CN), Jaccard (Jac), Cosine (COS), Leicht-Holme-Newman (LHN), Sorensen

Index (SSI), Hub-promoted Index (HPI), Preferential Attachment (PA), Hub-depressed Index (HDI). As we already defined the three CN similarities in the main text, we define here the metrics based on the seven additional classes.

Jaccard (Jac) similarity We define three metrics:

- Jaccard similarity (Jac):

$$s_{ij}^{Jac} = \frac{\sum_{\alpha} R_{i\alpha} R_{j\alpha}}{\sum_{\alpha} (R_{i\alpha} + R_{j\alpha} - R_{i\alpha} R_{j\alpha})}. \quad (5)$$

- Temporal Jaccard similarity with power-law time-lag decay (TJac):

$$s_{ij}^{TJac} = \frac{\sum_{\alpha} R_{i\alpha} R_{j\alpha} |t_{i\alpha} - t_{j\alpha}|^{-1} (1 - \delta_{t_{i\alpha}, t_{j\alpha}})}{\sum_{\alpha} (R_{i\alpha} + R_{j\alpha} - R_{i\alpha} R_{j\alpha})}. \quad (6)$$

- Temporal Jaccard similarity with one-step time-lag decay (TJac1):

$$s_{ij}^{TJac1} = \frac{\sum_{\alpha} R_{i\alpha} R_{j\alpha} \delta_{|t_{i\alpha} - t_{j\alpha}|, 1}}{\sum_{\alpha} (R_{i\alpha} + R_{j\alpha} - R_{i\alpha} R_{j\alpha})}. \quad (7)$$

Cosine (COS) similarity We define three metrics:

- Cosine similarity (COS):

$$s_{ij}^{COS} = \frac{\sum_{\alpha} R_{i\alpha} R_{j\alpha}}{\sqrt{\sum_{\alpha} R_{i\alpha} \sum_{\alpha} R_{j\alpha}}}. \quad (8)$$

- Temporal Cosine similarity with power-law time-lag decay (TCOS):

$$s_{ij}^{TCOS} = \frac{\sum_{\alpha} R_{i\alpha} R_{j\alpha} |t_{i\alpha} - t_{j\alpha}|^{-1} (1 - \delta_{t_{i\alpha}, t_{j\alpha}})}{\sqrt{\sum_{\alpha} R_{i\alpha} \sum_{\alpha} R_{j\alpha}}}. \quad (9)$$

- Temporal Cosine similarity with one-step time-lag decay (TCOS1):

$$s_{ij}^{TCOS1} = \frac{\sum_{\alpha} R_{i\alpha} R_{j\alpha} \delta_{|t_{i\alpha} - t_{j\alpha}|, 1}}{\sqrt{\sum_{\alpha} R_{i\alpha} \sum_{\alpha} R_{j\alpha}}}. \quad (10)$$

Leicht-Holme-Newman Index (LHN) similarity We define three metrics:

- Leicht-Holme-Newman Index similarity (LHN):

$$s_{ij}^{LHN} = \frac{\sum_{\alpha} R_{i\alpha} R_{j\alpha}}{\sum_{\alpha} R_{i\alpha} \sum_{\alpha} R_{j\alpha}}. \quad (11)$$

- Temporal Leicht-Holme-Newman Index similarity with power-law time-lag decay (TLHN):

$$s_{ij}^{TLHN} = \frac{\sum_{\alpha} R_{i\alpha} R_{j\alpha} |t_{i\alpha} - t_{j\alpha}|^{-1} (1 - \delta_{t_{i\alpha}, t_{j\alpha}})}{\sum_{\alpha} R_{i\alpha} \sum_{\alpha} R_{j\alpha}}. \quad (12)$$

- Temporal Leicht-Holme-Newman Index similarity with one-step time-lag decay (TLHN1):

$$s_{ij}^{TLHN1} = \frac{\sum_{\alpha} R_{i\alpha} R_{j\alpha} \delta_{|t_{i\alpha} - t_{j\alpha}|, 1}}{\sum_{\alpha} R_{i\alpha} \sum_{\alpha} R_{j\alpha}}. \quad (13)$$

Sørensen Index (SSI) similarity We define three metrics:

- Sørensen Index similarity (SSI):

$$s_{ij}^{SSI} = \frac{2 \times \sum_{\alpha} R_{i\alpha} R_{j\alpha}}{\sum_{\alpha} R_{i\alpha} + \sum_{\alpha} R_{j\alpha}}. \quad (14)$$

- Temporal Sørensen Index similarity with power-law time-lag decay (TSSI):

$$s_{ij}^{TSSI} = \frac{2 \times \sum_{\alpha} R_{i\alpha} R_{j\alpha} |t_{i\alpha} - t_{j\alpha}|^{-1} (1 - \delta_{t_{i\alpha}, t_{j\alpha}})}{\sum_{\alpha} R_{i\alpha} + \sum_{\alpha} R_{j\alpha}}. \quad (15)$$

- Temporal Sørensen Index similarity with one-step time-lag decay (TSSI1):

$$s_{ij}^{TSSI1} = \frac{2 \times \sum_{\alpha} R_{i\alpha} R_{j\alpha} \delta_{|t_{i\alpha} - t_{j\alpha}|, 1}}{\sum_{\alpha} R_{i\alpha} + \sum_{\alpha} R_{j\alpha}}. \quad (16)$$

Hub Promoted Index (HPI) similarity We define three metrics:

- Hub Promoted Index similarity (HPI):

$$s_{ij}^{HPI} = \frac{\sum_{\alpha} R_{i\alpha} R_{j\alpha}}{\min\{\sum_{\alpha} R_{i\alpha}, \sum_{\alpha} R_{j\alpha}\}} \quad (17)$$

- Temporal Hub Promoted Index similarity with power-law time-lag decay (THPI):

$$s_{ij}^{THPI} = \frac{\sum_{\alpha} R_{i\alpha} R_{j\alpha} |t_{i\alpha} - t_{j\alpha}|^{-1} (1 - \delta_{t_{i\alpha}, t_{j\alpha}})}{\min\{\sum_{\alpha} R_{i\alpha}, \sum_{\alpha} R_{j\alpha}\}} \quad (18)$$

- Temporal Hub Promoted Index similarity with one-step time-lag decay (THPI1):

$$s_{ij}^{THPI1} = \frac{\sum_{\alpha} R_{i\alpha} R_{j\alpha} \delta_{|t_{i\alpha} - t_{j\alpha}|, 1}}{\min\{\sum_{\alpha} R_{i\alpha}, \sum_{\alpha} R_{j\alpha}\}} \quad (19)$$

Hub Depressed Index (HDI) similarity We define three metrics:

- Hub Depressed Index similarity (HDI):

$$s_{ij}^{HDI} = \frac{\sum_{\alpha} R_{i\alpha} R_{j\alpha}}{\max\{\sum_{\alpha} R_{i\alpha}, \sum_{\alpha} R_{j\alpha}\}} \quad (20)$$

- Temporal Hub Depressed Index similarity with power-law time-lag decay (THDI):

$$s_{ij}^{THDI} = \frac{\sum_{\alpha} R_{i\alpha} R_{j\alpha} |t_{i\alpha} - t_{j\alpha}|^{-1} (1 - \delta_{t_{i\alpha}, t_{j\alpha}})}{\max\{\sum_{\alpha} R_{i\alpha}, \sum_{\alpha} R_{j\alpha}\}} \quad (21)$$

- Temporal Hub Depressed Index similarity with one-step time-lag decay (THDI1):

$$s_{ij}^{THDI1} = \frac{\sum_{\alpha} R_{i\alpha} R_{j\alpha} \delta_{|t_{i\alpha} - t_{j\alpha}|, 1}}{\max\{\sum_{\alpha} R_{i\alpha}, \sum_{\alpha} R_{j\alpha}\}} \quad (22)$$

Preferential Attachment (PA) similarity We define three metrics:

- Preferential Attachment similarity (PA):

$$s_{ij}^{PA} = \sum_{\alpha} R_{i\alpha} \sum_{\alpha} R_{j\alpha}. \quad (23)$$

- Temporal Preferential Attachment similarity with power-law time-lag decay (TPA):

$$s_{ij}^{TPA} = \sum_{\alpha} R_{i\alpha} \sum_{\alpha} R_{j\alpha} |t_{i\alpha} - t_{j\alpha}|^{-1} (1 - \delta_{t_{i\alpha}, t_{j\alpha}}). \quad (24)$$

- Temporal Preferential Attachment similarity with one-step time-lag decay (TPA1):

$$s_{ij}^{TPA1} = \sum_{\alpha} R_{i\alpha} \sum_{\alpha} R_{j\alpha} \delta_{|t_{i\alpha} - t_{j\alpha}|, 1}. \quad (25)$$

In all the temporal similarity methods above, we set $(t_{i\alpha} - t_{j\alpha})^{-1} = 0$ when $t_{i\alpha} = t_{j\alpha}$. Note that in the TC metrics, the factor $1 - \delta_{t_{i\alpha}, t_{j\alpha}}$ makes sure that events where $t_{i\alpha} = t_{j\alpha}$ do not contribute to the similarity. Indeed, when $t_{i\alpha} = t_{j\alpha}$, i is not the node that infected j ; therefore, i and j are unlikely to be connected in the networks. Note that in other problems such as link prediction and recommendation, the case $t_{i\alpha} = t_{j\alpha}$ may need to be treated differently.

4.2 SIR spreading dynamics

In the SIR model, each node is in one of the three states: Susceptible (S), Infected (I), Recovered (R). Each node has a probability f to be an initiator of the spreading process; therefore, there are $f \times N$ simultaneous initiators, on average, for each spreading process. At each time step, each infected node can infect each of its neighbors with probability β ; each infected node can recover with probability μ . For simplicity, we fix $\mu = 1$ (each node recovers one step after having been infected). The process ends when there are no more infected nodes in the system. For each empirical network, we run 50 independent realizations of the SIR dynamics. For each process α , we record the temporal list of the nodes infected by that process. The bipartite adjacency matrix R records which nodes were infected by which process: $R_{i\alpha} = 1$ if i has been infected by α , whereas $R_{i\alpha} = 0$ otherwise. If $R_{i\alpha} = 1$, the time step at which i was infected by α is recorded in $t_{i\alpha}$.

4.3 Generation of the synthetic networks

We use two well-known models for the generation of synthetic networks: the Barabási-Albert (BA) model [6], and the Small-World (SW) model [79].

Barabási-Albert (BA) We generate networks composed of $N = 500$ nodes. Our initial condition is a regular network where each node composed of $m_0 = 9$ nodes; each initial node has the degree equal to $\langle k \rangle = 5$. At each time step t , we add a new node to the network. The new node connects with $\langle k \rangle$ preexisting nodes; the probability that a preexisting node i is selected is proportional to its degree $k_i(t)$ at time t .

Small-World (SW) We start from a regular ring lattice composed of $N = 500$ nodes and degree $k = \langle k \rangle = 5$: we connect each of the N nodes with its nearest k neighbors. We rewire each link with probability p – in this work, we set $p = 0.1$. More specifically, for each node i , we select a node j from its neighbors and we extract a random number r from the uniform distribution in $(0, 1)$. If p is larger than r , we and remove the edge between node i and node j , we randomly select a node m , and we establish an edge between node i and node m .

Competing interests

The authors declare that they have no competing interests.

Author’s contribution

The work presented in this paper corresponds to a collaborative development by all authors. Conceptualization, H.L., M.S.M, and M-Y.Z.; Data Curation, M-K.L. and H.L.; Formal Analysis, H.L., M-K.L. and M.S.M.; Funding Acquisition, H.L. and M-Y.Z.; Methodology, M.S.M.; Resources, H.L. and M-Y.Z.; Software, M-K.L. and X-T.W.; Writing—Original Draft, M.S.M., M-K.L., M-Y.Z., X-T.W. and H.L.

Acknowledgements

We wish to thank Prof. Ginestra Bianconi and Prof. Chi Ho Yeung for providing us valuable suggestions. H.L. and M.Y.Z. acknowledge financial support from the National Natural Science Foundation of China (Grant Nos. 61803266, 61703281), Guangdong Province Natural Science Foundation (Grant Nos. 2016A030310051, 2017A030310374, 2017B030314073), Guangdong Pre-national project (Grant Nos. 2014GKXM054), Shenzhen Fundamental Research Foundation (JCYJ20160520162743717, JCYJ20150529164-656096), Natural Science Foundation of SZU (Grant No. 2016-24), Foundation for Distinguished Young Talents in Higher Education of Guangdong, China (Grant No. 2015K-QNCX143). MSM acknowledges the University of Zurich for support through the URPP Social Networks.

Supplementary

Data Description

Here we describe the 40 empirical networks analyzed in the main text.

- 1) **Facebook**: a social network which contains Facebook user–user friendships. [55]
- 2) **Jazz**: a music collaboration network obtained from the Red Hot Jazz Archive digital database. It includes 198 bands that performed between 1912 and 1940, with most of the bands from 1920 to 1940. [27]
- 3) **Residence hall**: a network which contains friendship ratings between 217 residents living at a residence hall located in the Australian National University campus. [23]
- 4) **E.coli**: a metabolic network of E.coli. [38]
- 5) **Physicians**: a network which captures the spreading paths of an innovation among 246 physicians in for towns in Illinois, Peoria, Bloomington, Quincy and Galesburg. [17]
- 6) **Neural**: a neural network in *C. elegans*. [20]
- 7) **Usair**: the US air transportation network that connects airport located in the United States.

- 8) **Dublin**: a network which describes the face-to-face behavior of people during the exhibition "infectious: stay away" in 2009 at the Science Gallery in Dublin. [36]
- 9) **Crim**: a network which connects persons who appeared in at least one crime case as either a suspect, a victim, a witness or both a suspect and victim at the same time.
- 10) **Caenorhabditis elegans**: a metabolic network of the roundworm *Caenorhabditis elegans*. [21]
- 11) **Email**: an email communication network at the University Rovira i Virgili in Tarragona in the south of Catalonia in Spain [32]
- 12) **Blogs**: a network which contains front-page hyperlinks between blogs in the context of the 2004 US election. [1]
- 13) **Air traffic control**: a network which was constructed from the USA's FAA (Federal Aviation Administration) National Flight Data Center (NFDC), Preferred Routes Database.
- 14) **Human protein**: a network of interactions between proteins in Humans (*Homo sapiens*), from the first large-scale study of protein-protein interactions in Human cells using a mass spectrometry-based approach. [71]
- 15) **Hamsterster friendships**: a network which contains friendships between users of the website hamsterster.com.
- 16) **UC Irvine messages**: a network which contains sent messages between the users of an online community of students from the University of California, Irvine. [62]
- 17) **Adolescent health**: a network which was created from a survey that took place in 1994/1995. [57]
- 18) **Advogato**: a network from an online community platform for developers of free software launched in 1999. [54]
- 19) **Euroroad**: an international E-road network, a road network located mostly in Europe. [76]
- 20) **Highschool**: a network which contains friendships between boys in a small high school in Illinois. [18]
- 21) **Hypertext**: a network of face-to-face contacts between the attendees of the ACM Hypertext 2009 conference. [36]
- 22) **IUI**: a network of the collaborations among the authors of papers published in *Informatika* and *Uporabna informatika*. [24]
- 23) **Amazon**: a network between web pages in amazon.com. [72]
- 24) **SCSC**: a network of collaborations between Slovenian computer scientists. [7]
- 25) **Zachary karate club**: the well-known Zachary karate club social network. [82]
- 26) **Polbooks**: a network of books about US politics published around the time of the 2004 presidential election and sold by the online bookseller Amazon.com. [2]
- 27) **Powergrid**: the power grid of the Western States of the United States of America. [78]
- 28) **Subelj**: the software class dependency network of the JUNG 2.0.1 and javax 1.6.0.7 libraries, namespaces edu.uci.ics.jung and java/javax.
- 29) **PPI**: a protein-protein interaction network. [75]
- 30) **Openflights**: a network which contains flights between airports of the world. [61]
- 31) **Bible**: a network which contains nouns (places and names) of the King James Version of the Bible and information about their co-occurrences. [84]
- 32) **Chicago**: a network on the road transportation of the Chicago region (USA). [22, 8]
- 33) **DNC email**: a network of emails in the 2016 Democratic National Committee email leak. [81]
- 34) **Word**: an adjacency network of common adjectives and nouns in the novel *David Copperfield* written by Charles Dickens. [60]
- 35) **Football**: a network of American football games between Division IA colleges during regular season Fall 2000. [26, 74]
- 36) **Little Rock Lake**: the food web of Little Rock Lake, Wisconsin in the United States of America. [52]
- 37) **Unicode**: a bipartite network denotes which languages are spoken in which countries. Here we transferred it to a unipartite network. [77]
- 38) **Netsci**: a coauthorship network between scientists who published on the topic of network science. [60]
- 39) **TAP**: a yeast protein binding network generated by tandem affinity purification experiments. [25]
- 40) **Slavko**: a small friendship network from an online website. [7]

SI Tables

Table 1: Properties of the analyzed empirical networks. N is the number of nodes. E is the number of edges. The parameter $\langle k \rangle$, refers to the average node degree. C is the average clustering coefficient. $\beta_c = \langle k \rangle / (\langle k^2 \rangle - \langle k \rangle)$ represents the critical value of the transmission probability in the SIR model in the mean-field scenario [64].

Network	N	E	$\langle k \rangle$	C	β_c	url
Zachary karate club (Zkc)	34	78	4.58	0.12	0.1688	url
Highschool (Highs)	70	366	10.45	0.29	0.1487	url
Polbooks (Polbs)	105	441	8.4	0.15	0.2067	url
Word	112	425	3.79	0.17	0.0783	url
Hypertext (Hypert)	113	20818	368.46	0.26	0.0392	url
Football (Footb)	115	1231	21.4	0.17	0.1623	url
Little Rock Lake (LRL)	183	2494	27.25	0.09	0.0229	url
Jazz	198	2742	27.69	0.62	0.0266	url
Residence hall (Rhall)	217	2672	24.62	0.24	0.0688	url
E.coli	230	695	6.04	0.22	0.0752	url
Physicians (Phys)	241	1098	9.11	0.13	0.1366	url
Neural	297	2359	15.88	0.12	0.049	url
USAir	332	2126	12.8	0.63	0.0231	url
Slavko	334	2218	13.28	0.17	0.0791	url
Netsci	379	914	4.82	0.74	0.1424	url
Dublin	410	2765	13.48	0.30	0.1044	url
Caenorhabditis elegans (Cae)	453	4596	10.15	0.07	0.0465	url
Unicode (Unic)	767	1255	3.27	0.01	0.0455	url
Scsc	961	1925	4.01	0.02	0.2033	url
Email	1133	5451	9.62	0.22	0.0565	url
Euroroad (Eroad)	1174	1417	2.41	0.01	0.1563	url
Blogs	1224	19025	31.08	0.14	0.0123	url
Air traffic control (Air.tra)	1226	2615	4.26	0.02	0.2353	url
TAP	1373	6833	9.96	0.53	0.0651	url
Crim	1380	1476	2.13	0.1	0.0458	url
Chicago (Chic)	1467	1298	1.76	0	0.1411	url
Human protein (HP)	1706	6207	7.27	0.02	0.0653	url
Bible	1773	16401	18.5	0.1	0.1299	url
Hamsterster friendships (HF)	1858	12534	13.49	0	0.0217	url
UC Irvine messages (UC.irv)	1899	59835	63.01	0.04	0.0317	url
DNC emails (DNC)	2029	39264	38.70	0.06	0.0164	url
IUI	2288	4190	3.66	0.03	0.3068	url
PPI	2375	11693	9.84	0.3	0.0301	url
Adolescent health (Health)	2539	12969	10.21	0.10	0.1408	url
Amazon (Ama)	2880	5037	3.49	0.01	0.1651	url
Facebook (Faceb)	2888	2981	2.06	0	0.1879	url
Openflights (Oflys)	2939	30501	20.75	0.39	0.0184	url
Powergrid (Pgrid)	4941	6594	2.66	0.01	0.1175	url
Subelj	6434	150985	46.93	0.09	0.0513	url
Advogato (Adv)	6541	51127	7.82	0.11	0.0171	url

Table 2: Basic properties of real networks and the performance of the COS, TCOS, TCOS1, SS, TSS, TSS1, LHN, TLHN, TLHN1, HD, THD and THD1 methods on these networks, based on the AUC metric. The parameters are set as $\beta = 4\beta_c$ and $f = 0.5$. We select a relatively large β because the performance difference between traditional similarity metric and temporal similarity metric becomes more significant under large β . The similarity method with the best performance in each network is highlighted in bold font. The results are averaged over 50 independent realizations.

Network	Basic properties		AUC											
	N	E	COS	TCOS	TCOS1	SSI	TSSI	TSS1	LHN	TLHN	TLHN1	HDI	THDI	THD1
Zkc	34	78	0.6683	0.6816	0.6811	0.6659	0.6797	0.6835	0.6585	0.6770	0.6776	0.6604	0.6782	0.6775
Highs	70	366	0.7614	0.8532	0.8525	0.7600	0.8491	0.8490	0.6396	0.8367	0.8367	0.7500	0.8411	0.8410
Polbs	105	441	0.7201	0.7206	0.7199	0.7073	0.7096	0.7101	0.6552	0.6711	0.6714	0.6888	0.7002	0.7011
Word	112	425	0.8413	0.9350	0.9506	0.7821	0.8898	0.9305	0.8311	0.9033	0.9396	0.8056	0.8937	0.9313
Hypert	113	20818	0.5314	0.5447	0.5438	0.5219	0.5356	0.5352	0.5446	0.5491	0.5509	0.5137	0.5271	0.5271
Footb	115	1231	0.6789	0.7216	0.7216	0.6557	0.6945	0.6941	0.6813	0.7116	0.7108	0.6373	0.6750	0.6741
LRL	183	2494	0.6462	0.6488	0.6491	0.6452	0.6482	0.6481	0.6431	0.6469	0.6469	0.6464	0.6488	0.6488
Jazz	198	2742	0.8312	0.8650	0.8783	0.8211	0.8609	0.8753	0.7563	0.7875	0.8218	0.7942	0.8487	0.8686
Rhall	217	2672	0.7103	0.8683	0.8682	0.6856	0.7954	0.7956	0.7094	0.8308	0.8311	0.7030	0.8344	0.8346
E. coli	230	695	0.9018	0.9726	0.9822	0.8876	0.9659	0.9797	0.7924	0.8999	0.9307	0.8965	0.9504	0.9712
Phys	241	1098	0.8610	0.8737	0.8738	0.8587	0.8717	0.8720	0.6278	0.8375	0.8377	0.8521	0.8672	0.8675
Neural	297	2359	0.7314	0.8266	0.8380	0.7287	0.8098	0.8303	0.7174	0.7865	0.8068	0.7213	0.7920	0.8176
USAir	332	2126	0.9135	0.9435	0.9539	0.9089	0.9365	0.9474	0.7852	0.8199	0.8273	0.9023	0.9289	0.9390
Slavko	334	2218	0.7711	0.7686	0.7683	0.7596	0.7615	0.7609	0.7552	0.7576	0.7574	0.7508	0.7549	0.7549
Netsci	379	914	0.9225	0.9755	0.9752	0.9198	0.9760	0.9760	0.9138	0.9635	0.9632	0.8987	0.9810	0.9807
Dublin	410	2765	0.7959	0.8460	0.8462	0.7322	0.8427	0.8430	0.6985	0.7567	0.7567	0.7735	0.8226	0.8231
Cae	453	4596	0.7122	0.7369	0.7348	0.7062	0.7202	0.7231	0.6794	0.7161	0.7190	0.6992	0.7160	0.7163
Unic	767	1255	0.6018	0.6020	0.6020	0.6019	0.6021	0.6023	0.6022	0.6021	0.6020	0.6021	0.6021	0.6020
Scsc	961	1925	0.8158	0.8160	0.8161	0.8151	0.8159	0.8159	0.8158	0.8159	0.8160	0.8151	0.8162	0.8154
Email	1133	5451	0.8567	0.9725	0.9946	0.8423	0.9617	0.9925	0.8341	0.9407	0.9823	0.8389	0.9470	0.9797
Eroad	1174	1417	0.8942	0.9186	0.9185	0.8943	0.9146	0.9148	0.8114	0.9177	0.9172	0.8925	0.9136	0.9136
Blogs	1224	19025	0.8431	0.8580	0.8581	0.8401	0.8493	0.8494	0.8342	0.8451	0.8452	0.8269	0.8391	0.8390
Air.tra	1226	2615	0.8439	0.8640	0.8643	0.8257	0.8533	0.8537	0.8330	0.8568	0.8571	0.8527	0.8652	0.8652
TAP	1373	6833	0.8964	0.9924	0.9983	0.8757	0.9906	0.9982	0.8423	0.9902	0.9980	0.8558	0.9814	0.9966
Crim	1380	1476	0.7959	0.8444	0.8446	0.6986	0.7556	0.7558	0.7870	0.8297	0.8298	0.7738	0.8219	0.8220
Chic	1467	1298	0.6513	0.6515	0.6517	0.6517	0.6516	0.6516	0.6517	0.6519	0.6518	0.6519	0.6517	0.6518
HP	1706	6207	0.9376	0.9833	0.9831	0.8802	0.9371	0.9373	0.9274	0.9756	0.9760	0.9081	0.9720	0.9723
Bible	1773	16401	0.7413	0.7551	0.7555	0.7131	0.7253	0.7245	0.7056	0.7303	0.7310	0.6822	0.7005	0.7007
HF	1858	12534	0.7726	0.7768	0.7770	0.7673	0.7714	0.7717	0.7708	0.7737	0.7738	0.7701	0.7737	0.7733
Uc.irv	1899	59835	0.8996	0.9471	0.9471	0.8973	0.9254	0.9258	0.8952	0.9265	0.9266	0.8956	0.9123	0.9127
DNC	2029	39264	0.9613	0.9618	0.9619	0.9608	0.9613	0.9614	0.9372	0.9432	0.9437	0.9603	0.9612	0.9611
IUI	2288	4190	0.8276	0.8277	0.8274	0.8281	0.8268	0.8278	0.8287	0.8278	0.8283	0.8275	0.8271	0.8278
PPI	2375	11693	0.9349	0.9747	0.9747	0.9336	0.9707	0.9706	0.7811	0.9250	0.9249	0.9314	0.9652	0.9650
Health	2539	12969	0.7561	0.8970	0.8979	0.7502	0.8886	0.8890	0.7896	0.9339	0.9347	0.7444	0.8724	0.8733
Ama	2880	5037	0.6535	0.9172	0.9178	0.6502	0.9172	0.9172	0.6531	0.9168	0.9160	0.6314	0.9138	0.9140
Faceb	2888	2981	0.6789	0.7216	0.7216	0.6557	0.6945	0.6941	0.6813	0.7116	0.7108	0.6373	0.6750	0.6741
Ofigs	2939	30501	0.9384	0.9581	0.9578	0.9311	0.9505	0.9507	0.6979	0.7957	0.7957	0.9239	0.9432	0.9433
Pgrid	4941	6594	0.8927	0.8928	0.8929	0.8922	0.8929	0.8926	0.8916	0.8928	0.8927	0.8917	0.8928	0.8927
Subelj	6434	150985	0.6284	0.7016	0.7016	0.6353	0.6745	0.6741	0.6616	0.6916	0.6908	0.6178	0.6550	0.6541
Adv	6541	51127	0.9104	0.9269	0.9270	0.9099	0.9242	0.9249	0.7914	0.8373	0.8361	0.9050	0.9180	0.9173

Table 3: Basic properties of real networks and the performance of the COS, TCOS, TCOS1, SS, TSS, TSS1, LHN, TLHN, TLHN1, HD, THD and THD1 methods on these networks, based on the precision metric. The parameters are set as $\beta = 4 \beta_c$ and $f = 0.5$. We select a relatively large β because the performance difference between traditional similarity metric and temporal similarity metric becomes more significant under large β . The similarity method with the best performance in each network is highlighted in bold font. The results are averaged over 50 independent realizations.

Network	Basic properties		Precision											
	N	E	COS	TCOS	TCOS1	SSI	TSSI	TSS1	LHN	TLHN	TLHN1	HDI	THDI	THD1
Zkc	34	78	0.207	0.235	0.236	0.209	0.237	0.230	0.193	0.214	0.221	0.209	0.224	0.230
Highs	70	366	0.365	0.535	0.610	0.365	0.536	0.611	0.181	0.474	0.571	0.357	0.537	0.620
Polbs	105	441	0.217	0.217	0.241	0.217	0.213	0.234	0.138	0.172	0.186	0.205	0.198	0.220
Word	112	425	0.313	0.568	0.624	0.307	0.548	0.610	0.241	0.320	0.390	0.297	0.489	0.562
Hypert	113	20818	0.221	0.239	0.244	0.215	0.231	0.240	0.220	0.231	0.233	0.202	0.221	0.228
Footb	115	1231	0.224	0.286	0.320	0.212	0.267	0.306	0.156	0.201	0.232	0.176	0.233	0.278
LRL	183	2494	0.282	0.310	0.287	0.275	0.305	0.286	0.259	0.294	0.287	0.270	0.302	0.285
Jazz	198	2742	0.434	0.531	0.538	0.426	0.528	0.537	0.304	0.342	0.407	0.405	0.509	0.531
Rhall	217	2672	0.189	0.462	0.565	0.181	0.340	0.457	0.189	0.379	0.506	0.185	0.408	0.520
E. coli	230	695	0.323	0.584	0.652	0.348	0.558	0.626	0.278	0.303	0.354	0.317	0.514	0.579
Phys	241	1098	0.315	0.460	0.464	0.162	0.275	0.353	0.309	0.439	0.468	0.284	0.427	0.453
Neural	297	2359	0.178	0.327	0.376	0.152	0.312	0.369	0.124	0.243	0.295	0.142	0.271	0.335
USAir	332	2126	0.561	0.555	0.541	0.554	0.549	0.536	0.219	0.234	0.339	0.526	0.532	0.533
Slavko	334	2218	0.253	0.261	0.258	0.243	0.254	0.253	0.132	0.162	0.175	0.215	0.229	0.236
Netsci	379	914	0.371	0.581	0.771	0.370	0.583	0.773	0.279	0.0517	0.628	0.359	0.579	0.788
Dublin	410	2765	0.203	0.355	0.361	0.115	0.212	0.279	0.199	0.343	0.370	0.176	0.319	0.348
Cae	453	4596	0.141	0.229	0.236	0.139	0.224	0.233	0.077	0.101	0.114	0.112	0.195	0.214
Unic	767	1255	0.104	0.156	0.153	0.103	0.152	0.153	0.098	0.141	0.152	0.101	0.148	0.152
Sesc	961	1925	0.233	0.271	0.279	0.230	0.266	0.272	0.179	0.214	0.234	0.216	0.250	0.258
Email	1133	5451	0.467	0.568	0.766	0.442	0.503	0.707	0.145	0.206	0.341	0.256	0.397	0.581
Eroad	1174	1417	0.230	0.424	0.425	0.227	0.424	0.425	0.137	0.185	0.259	0.228	0.413	0.414
Blogs	1224	19025	0.173	0.242	0.287	0.166	0.216	0.246	0.173	0.226	0.254	0.171	0.226	0.256
Air.tra	1226	2615	0.186	0.374	0.402	0.179	0.383	0.403	0.056	0.132	0.156	0.158	0.366	0.367
TAP	1373	6833	0.232	0.635	0.734	0.215	0.617	0.717	0.158	0.502	0.713	0.187	0.590	0.678
Crim	1380	1476	0.034	0.227	0.228	0.041	0.228	0.228	0.077	0.229	0.287	0.041	0.228	0.231
Chic	1467	1298	0.294	0.303	0.304	0.298	0.303	0.304	0.287	0.302	0.304	0.298	0.303	0.304
HP	1706	6207	0.135	0.221	0.312	0.122	0.189	0.246	0.136	0.199	0.255	0.131	0.198	0.255
Bible	1773	16401	0.152	0.208	0.213	0.148	0.207	0.216	0.043	0.052	0.056	0.119	0.184	0.210
HF	1858	12534	0.090	0.157	0.195	0.067	0.075	0.086	0.086	0.127	0.159	0.071	0.122	0.151
Uc.irv	1899	59835	0.176	0.370	0.354	0.113	0.257	0.324	0.171	0.374	0.371	0.155	0.339	0.342
DNC	2029	39264	0.373	0.376	0.373	0.372	0.375	0.374	0.013	0.019	0.019	0.362	0.370	0.373
IUI	2288	4190	0.140	0.196	0.229	0.143	0.196	0.205	0.351	0.303	0.323	0.142	0.183	0.199
Health	2539	12969	0.025	0.533	0.618	0.025	0.530	0.616	0.039	0.327	0.478	0.025	0.418	0.599
Ama	2880	5037	0.008	0.015	0.015	0.009	0.013	0.014	0.005	0.014	0.014	0.007	0.013	0.014
Faceb	2888	2981	0.224	0.286	0.320	0.212	0.268	0.306	0.157	0.201	0.232	0.176	0.234	0.278
Ofigs	2939	30501	0.248	0.321	0.368	0.248	0.320	0.363	0.021	0.028	0.031	0.244	0.293	0.335
Pgrid	4941	6594	0.185	0.311	0.312	0.183	0.310	0.311	0.122	0.206	0.228	0.184	0.301	0.302
Subelj	6434	150985	0.067	0.124	0.130	0.065	0.120	0.125	0.016	0.046	0.051	0.066	0.114	0.115
Adv	6541	51127	0.061	0.155	0.322	0.060	0.151	0.288	0.002	0.069	0.091	0.061	0.120	0.240

SI FIGURES

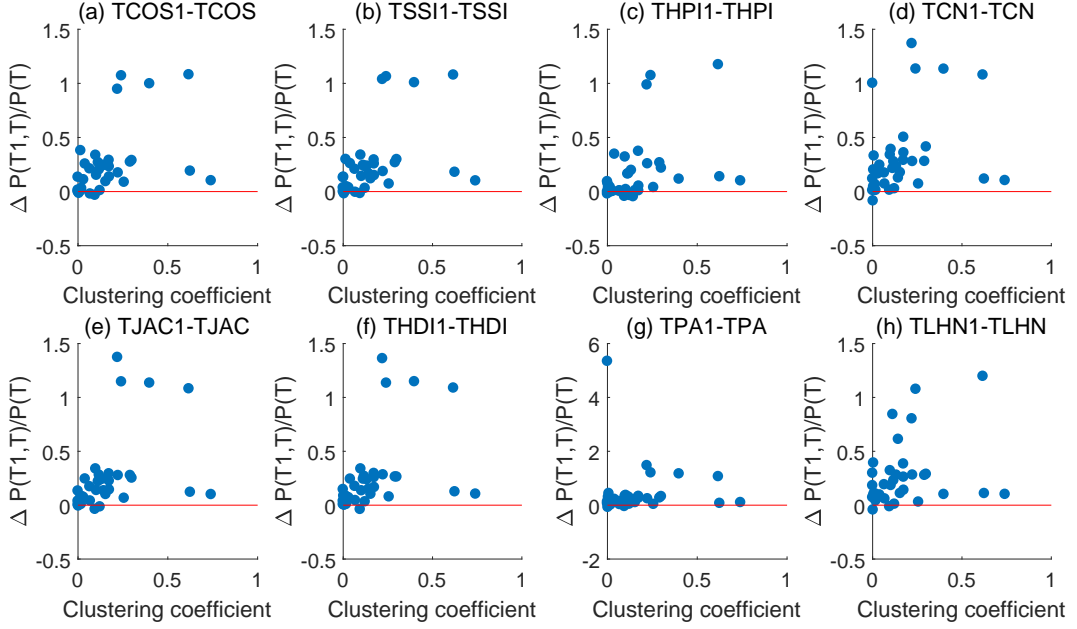


Figure S1: Results for the SIR spreading dynamics: Reconstruction precision relative difference $\Delta P(T1, T)/P(T) = (P(T1) - P(T))/P(T)$ as a function of the network clustering coefficient (see Methods for the definition). Each dot represents an empirical network, we totally analyzed 40 empirical network. We use $f = 0.5, \beta = 8\beta_c$ here, where $\beta_c = \langle k \rangle / (\langle k^2 \rangle - \langle k \rangle)$. The results are averaged over 50 independent realizations.

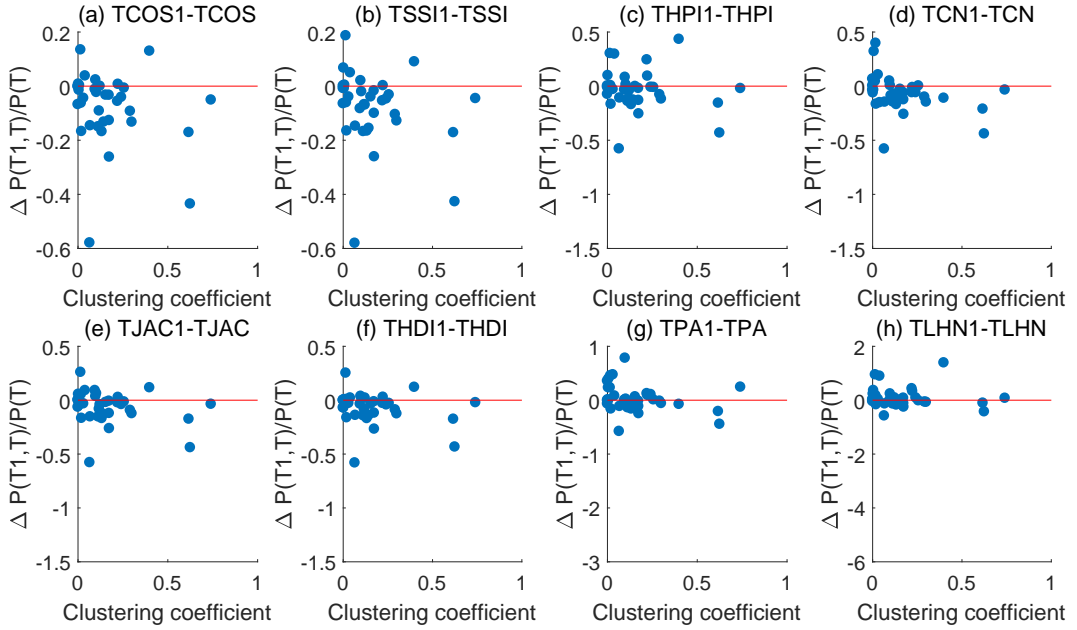


Figure S2: Results for the SIR spreading dynamics: Reconstruction precision relative difference $\Delta P(T1, T)/P(T) = (P(T1) - P(T))/P(T)$ as a function of the network clustering coefficient (see Methods for the definition). Each dot represents an empirical network, we totally analyzed 40 empirical network. We use $f = 0.5, \beta = \beta_c$ here, where $\beta_c = \langle k \rangle / (\langle k^2 \rangle - \langle k \rangle)$. The results are averaged over 50 independent realizations.

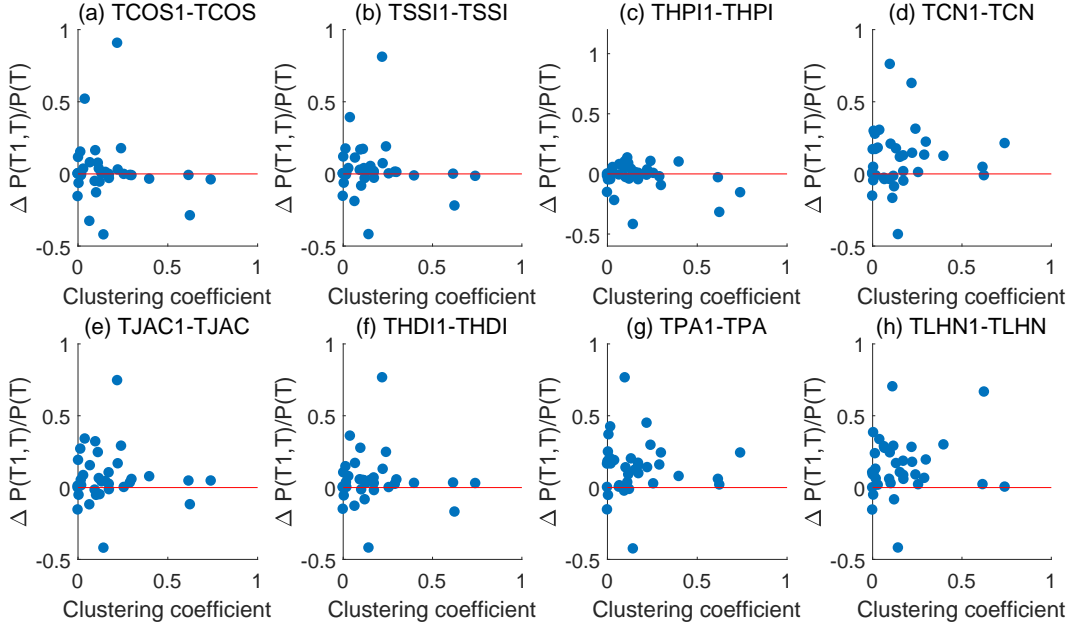


Figure S3: Results for the SIR spreading dynamics: Reconstruction precision relative difference $\Delta P(T1, T)/P(T) = (P(T1) - P(T))/P(T)$ as a function of the network clustering coefficient (see Methods for the definition). Each dot represents an empirical network, we totally analyzed 40 empirical network. We use $f = 0.5, \beta = 2\beta_c$ here, where $\beta_c = \langle k \rangle / (\langle k^2 \rangle - \langle k \rangle)$. The results are averaged over 50 independent realizations.

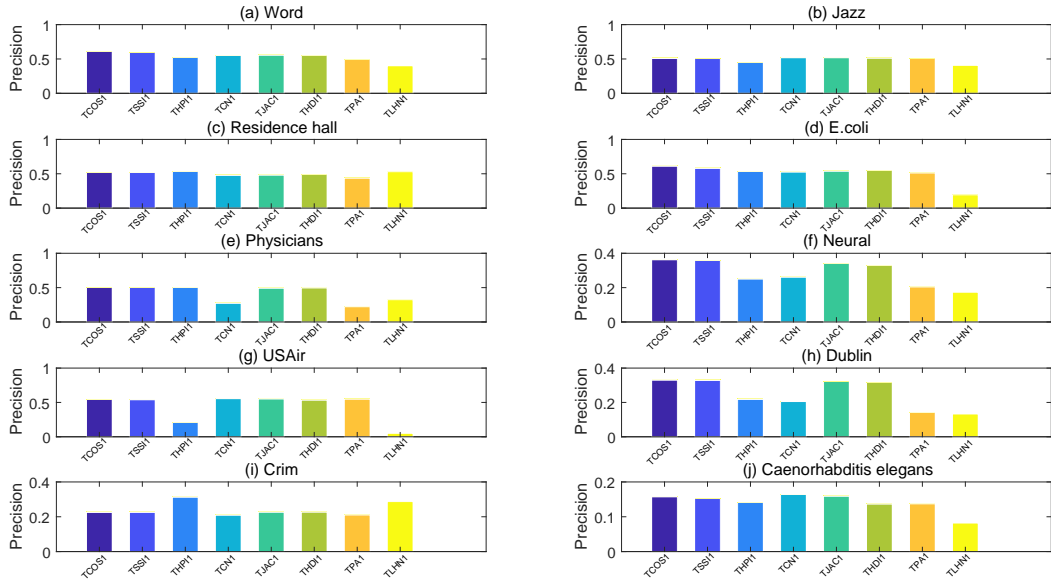


Figure S4: Results for the SIR spreading dynamics: Reconstruction precision for 10 networks. Each panel represents the performance of the 8 TX1 metrics for a single network. This figure shows the results for $\beta = 4\beta_c$, where $\beta_c = \langle k \rangle / (\langle k^2 \rangle - \langle k \rangle)$, and $f = 0.5$. The results are averaged over 50 independent realizations.

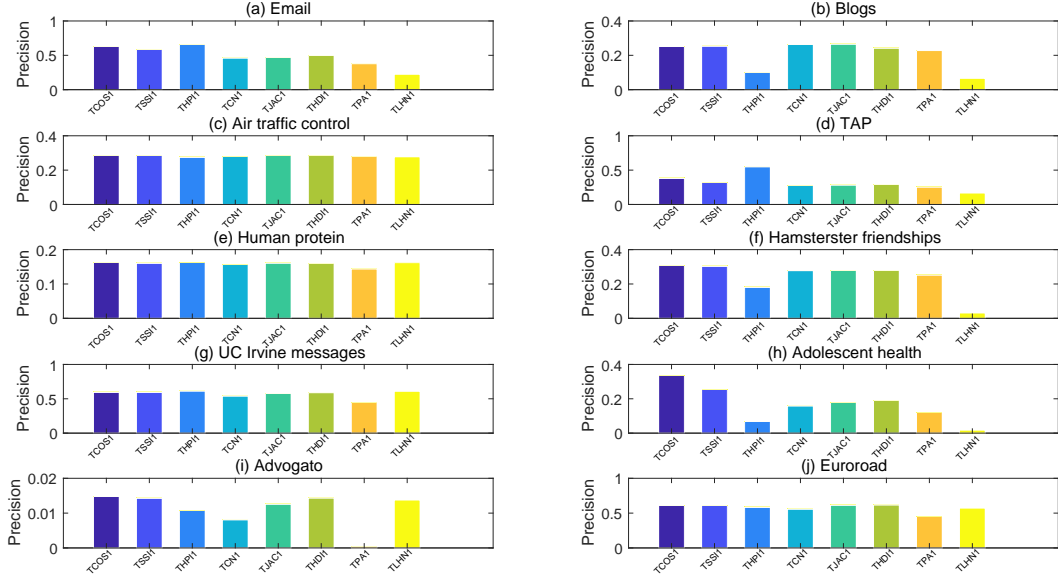


Figure S5: Results for the SIR spreading dynamics: Reconstruction precision for 10 networks. Each panel is the performance of the 8 TX1 metrics for a single network. This figure shows the results for $\beta = 4\beta_c$, where $\beta_c = \langle k \rangle / (\langle k^2 \rangle - \langle k \rangle)$, and $f = 0.5$. The results are averaged over 50 independent realizations.

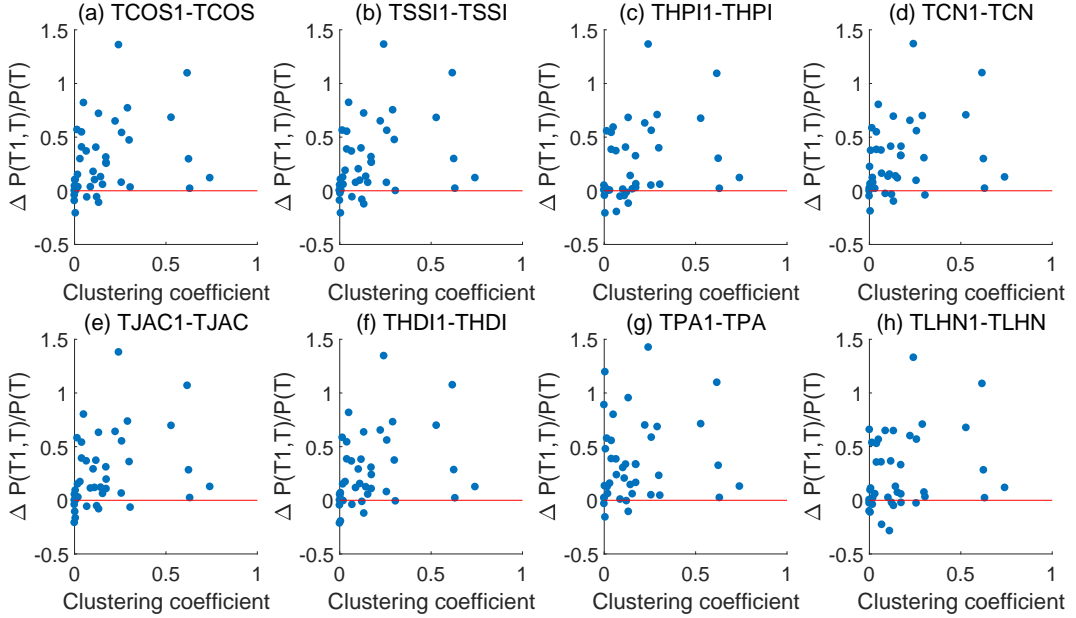


Figure S6: Results for the SI spreading dynamics [3, 70]. The SI model is a special case of the SIR model where each infected node cannot recover ($\mu = 0$). Reconstruction precision relative difference $\Delta P(T1, T)/P(T) = (P(T1) - P(T))/P(T)$ as a function of the network clustering coefficient. Each dot represents an empirical network; we analyzed 40 empirical contact networks. For all classes of similarity, almost all the empirical networks fall above the $P(T1)=P(T)$ red line; the only exceptions are some of the networks with low clustering coefficient. We used $\beta = 4\langle k \rangle / (\langle k^2 \rangle - \langle k \rangle)$, and $f = 0.5$ here. The results are averaged over 50 independent realizations.

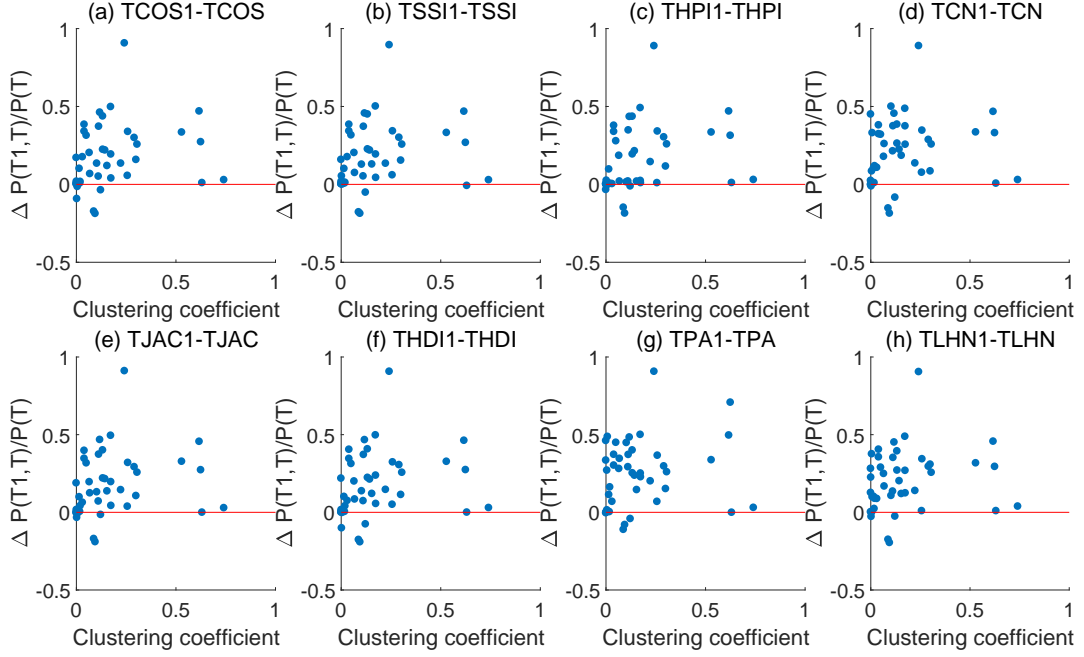


Figure S7: Results for the LTM (Linear Threshold Model) [12, 30]. In the LTM, we replace a link by a pair of directed links, $A \rightarrow B$ and $B \rightarrow A$, and every directed edge has a weight $1/k_i^{ind}$, where k_i^{ind} represents the indegree of node i . Each node is in one among two possible states, Inactive or Active. A node activates if $\sum_j A_{ij}W_{ij} \geq \theta_i$, where θ_i represents node i 's threshold. In our simulations, we start from an initial condition with a fraction $f = 0.5$ of randomly-selected Active nodes, and we set $\theta_i = \theta = 0.1$. We show here the reconstruction precision relative difference $\Delta P(T1, T)/P(T) = (P(T1) - P(T))/P(T)$ as a function of the network clustering coefficient. Each dot represents an empirical network; we analyzed 40 empirical contact networks. For all classes of similarity, almost all the empirical networks fall above the $P(T1)=P(T)$ red line; the only exceptions are some of the networks with low clustering coefficient. The results are averaged over 50 independent realizations.

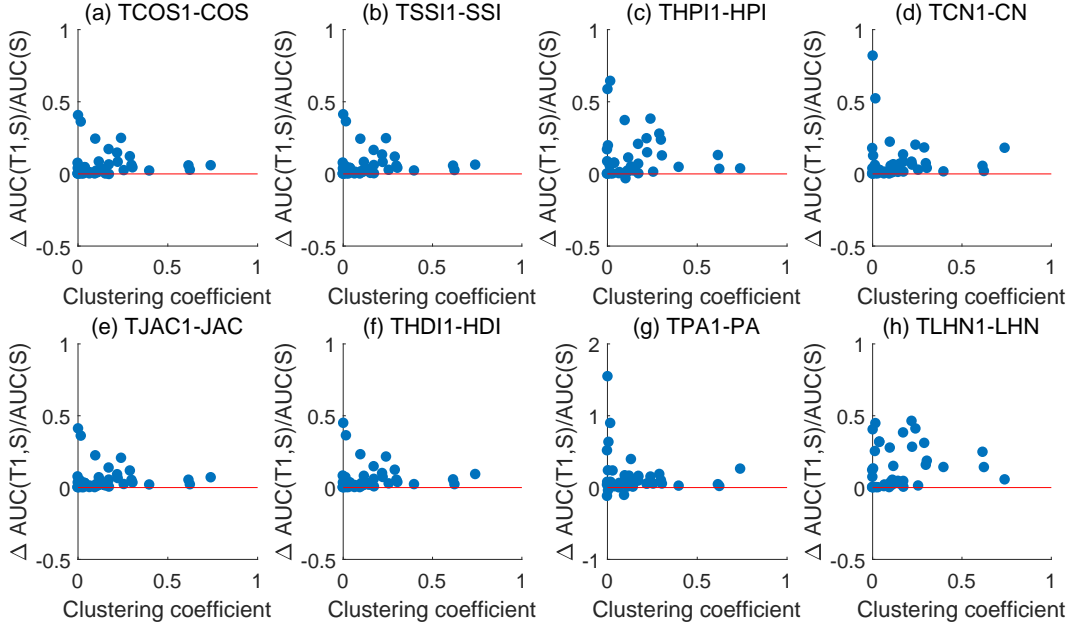


Figure S8: Results for the SIR spreading dynamics: Reconstruction AUC relative difference $\Delta AUC(T1, S)/AUC(S) = (AUC(T1) - AUC(S))/AUC(S)$ as a function of the network clustering coefficient (see Methods for the definition). Each dot represents an empirical network, we totally analyzed 40 empirical network. We use $f = 0.5$, $\beta = 4\beta_c$ here, where $\beta_c = \langle k \rangle / (\langle k^2 \rangle - \langle k \rangle)$. The results are averaged over 50 independent realizations.

References

- [1] Lada A Adamic and Natalie Glance. The Political Blogosphere and the 2004 US Election: Divided they Blog. In *Proceedings of the 3rd International Workshop on Link Discovery*, pages 36–43. ACM, 2005.
- [2] Mohammad Al Hasan and Mohammed J Zaki. A survey of link prediction in social networks. In *Social network data analytics*, pages 243–275. Springer, 2011.
- [3] Roy M Anderson and Robert M May. *Infectious diseases of humans: dynamics and control*. Oxford university press, Oxford, England, UK, 1992.
- [4] Lars Backstrom and Jure Leskovec. Supervised random walks: predicting and recommending links in social networks. In *Proceedings of the 4th ACM International Conference on Web Search and Data Mining*, pages 635–644. ACM, 2011.
- [5] Eytan Bakshy, Itamar Rosenn, Cameron Marlow, and Lada Adamic. The role of social networks in information diffusion. In *Proceedings of the 21st International Conference on World Wide Web*, pages 519–528. ACM, 2012.
- [6] Albert-László Barabási and Réka Albert. Emergence of scaling in random networks. *Science*, 286(5439):509–512, 1999.
- [7] Neli Blagus, Lovro Šubelj, and Marko Bajec. Self-similar scaling of density in complex real-world networks. *Physica A*, 391(8):2794–2802, 2012.
- [8] D. E. Boyce, K. S. Chon, M. E. Ferris, Y. J. Lee, K-T. Lin, and R. W. Eash. Implementation and evaluation of combined models of urban travel and location on a sketch planning network. *Chicago Area Transportation Study*, pages xii + 169, 1985.
- [9] Dirk Brockmann and Dirk Helbing. The hidden geometry of complex, network-driven contagion phenomena. *Science*, 342(6164):1337–1342, 2013.
- [10] Carlo Vittorio Cannistraci, Gregorio Alanis-Lobato, and Timothy Ravasi. From link-prediction in brain connectomes and protein interactomes to the local-community-paradigm in complex networks. *Sci. Rep.*, 3:1613, 2013.

- [11] Wei Chen, Hongzhi Yin, Weiqing Wang, Lei Zhao, and Xiaofang Zhou. Effective and efficient user account linkage across location based social networks. In *Proceedings of the 34th IEEE International Conference on Data Engineering*, pages 1085–1096. IEEE, 2018.
- [12] Wei Chen, Yifei Yuan, and Li Zhang. Scalable influence maximization in social networks under the linear threshold model. In *Proceedings of the 10th IEEE International Conference on Data Mining*, pages 88–97. IEEE, 2010.
- [13] Yuanfang Chen, Noel Crespi, Antonio M Ortiz, and Lei Shu. Reality mining: A prediction algorithm for disease dynamics based on mobile big data. *Inf. Sci.*, 379:82–93, 2017.
- [14] Giulio Cimini, Tiziano Squartini, Diego Garlaschelli, and Andrea Gabrielli. Systemic risk analysis on reconstructed economic and financial networks. *Sci. Rep.*, 5:15758, 2015.
- [15] Valerio Ciotti, Moreno Bonaventura, Vincenzo Nicosia, Pietro Panzarasa, and Vito Latora. Homophily and missing links in citation networks. *EPJ Data Sci.*, 5(1):7, 2016.
- [16] Aaron Clauset, Christopher Moore, and Mark EJ Newman. Hierarchical structure and the prediction of missing links in networks. *Nature*, 453(7191):98, 2008.
- [17] James Coleman, Elihu Katz, and Herbert Menzel. The diffusion of an innovation among physicians. *Sociometry*, pages 253–270, 1957.
- [18] James Samuel Coleman. Introduction to mathematical sociology. *London Free Press Glencoe*, 1964.
- [19] Simone Daminelli, Josephine Maria Thomas, Claudio Durán, and Carlo Vittorio Cannistraci. Common neighbours and the local-community-paradigm for topological link prediction in bipartite networks. *New J. Phys.*, 17(11):113037, 2015.
- [20] Jordi Duch and Alex Arenas. Community detection in complex networks using extremal optimization. *Phys. Rev. E Stat. Nonlin. Soft*, 72(2):027104, 2005.
- [21] Jordi Duch and Alex Arenas. Community detection in complex networks using extremal optimization. *Phys. Rev. E Stat. Nonlin. Soft*, 72(2):027104, 2005.
- [22] R. W. Eash, K. S. Chon, Y. J. Lee, and D. E. Boyce. Equilibrium traffic assignment on an aggregated highway network for sketch planning. *Transportation Research Record*, 994:30–37, 1983.
- [23] Linton Clarke Freeman, Cynthia Marie Webster, and Deirdre M Kirke. Exploring social structure using dynamic three-dimensional color images. *Social Networks*, 20(2):109–118, 1998.
- [24] Zhong-Ke Gao, Yu-Xuan Yang, Peng-Cheng Fang, Ning-De Jin, Cheng-Yi Xia, and Li-Dan Hu. Multi-frequency complex network from time series for uncovering oil-water flow structure. *Sci. Rep.*, 5:8222, 2015.
- [25] Anne-Claude Gavin, Patrick Aloy, Paola Grandi, Roland Krause, Markus Boesche, Martina Marzioch, Christina Rau, Lars Juhl Jensen, Sonja Bastuck, Birgit Dümpelfeld, et al. Proteome survey reveals modularity of the yeast cell machinery. *Nature*, 440(7084):631, 2006.
- [26] M Girvan and MEJ Newman. Network of american football games between division ia colleges during regular season fall 2000. *Proc. Natl. Acad. Sci.*, 99:7821–7826, 2002.
- [27] Pablo M. Gleiser and Leon Danon. Community structure in jazz. *Advances in Complex Systems*, 6(4):565–573, 2003.
- [28] Manuel Gomez-Rodriguez, Jure Leskovec, and Andreas Krause. Inferring networks of diffusion and influence. *ACM Trans. Knowl. Discov. Data*, 5(4):21, 2012.
- [29] Maoguo Gong, Jianan Yan, Bo Shen, Lijia Ma, and Qing Cai. Influence maximization in social networks based on discrete particle swarm optimization. *Inf. Sci.*, 367:600–614, 2016.
- [30] Mark Granovetter. Threshold models of collective behavior. *Am. J. Sociol.*, 83(6):1420–1443, 1978.
- [31] Aditya Grover and Jure Leskovec. Node2vec: Scalable feature learning for networks. In *Proceedings of the 22nd ACM SIGKDD International Conference on Knowledge Discovery and Data Mining*, pages 855–864. ACM, 2016.
- [32] Roger Guimerà, Leon Danon, Albert Dàaz-Guilera, Francesc Giralt, and Alex Arenas. Self-similar community structure in a network of human interactions. *Phys. Rev. E Stat. Nonlin. Soft*, 68(6):065103, 2003.
- [33] Roger Guimerà and Marta Sales-Pardo. Missing and spurious interactions and the reconstruction of complex networks. *Proc. Natl. Acad. Sci.*, 106(52):22073–22078, 2009.
- [34] Petter Holme and Jari Saramäki. Temporal networks. *Phys. Rep.*, 519(3):97–125, 2012.

- [35] Zan Huang and Dennis KJ Lin. The time-series link prediction problem with applications in communication surveillance. *INFORMS J. Comput.*, 21(2):286–303, 2009.
- [36] Lorenzo Isella, Juliette Stehlé, Alain Barrat, Ciro Cattuto, Jean-François Pinton, and Wouter Van den Broeck. What’s in a crowd? analysis of face-to-face behavioral networks. *J. Theor. Biol.*, 271(1):166–180, 2011.
- [37] Paul Jaccard. Étude comparative de la distribution florale dans une portion des alpes et des jura. *Bull. Soc. Vaudoise Sci. Nat.*, 37:547–579, 1901.
- [38] Hawoong Jeong, Bálint Tombor, Réka Albert, Zoltan N Oltvai, and A-L Barabási. The large-scale organization of metabolic networks. *Nature*, 407(6804):651, 2000.
- [39] Leo Katz. A new status index derived from sociometric analysis. *Psychometrika*, 18(1):39–43, 1953.
- [40] David Kempe, Jon Kleinberg, and Éva Tardos. Maximizing the spread of influence through a social network. In *Proceedings of the 9th ACM SIGKDD International Conference on Knowledge Discovery and Data Mining*, pages 137–146. ACM, 2003.
- [41] István A Kovács, Katja Luck, Kerstin Spirohn, Yang Wang, Carl Pollis, Sadie Schlabach, Wenting Bian, Dae-Kyum Kim, Nishka Kishore, and Tong Hao. Network-based prediction of protein interactions. *bioRxiv*, page 275529, 2018.
- [42] Danielle H Lee and Peter Brusilovsky. How to measure information similarity in online social networks: A case study of citeulike. *Inf. Sci.*, 418:46–60, 2017.
- [43] Elizabeth A Leicht, Petter Holme, and Mark EJ Newman. Vertex similarity in networks. *Phys. Rev. E*, 73(2):026120, 2006.
- [44] Rong-Hua Li, Jeffery Xu Yu, Xin Huang, and Hong Cheng. Robust reputation-based ranking on bipartite rating networks. In *Proceedings of the 2012 SIAM International Conference on Data Mining*, pages 612–623. SIAM, 2012.
- [45] Rong-Hua Li, Jeffrey Xu Yu, and Jianquan Liu. Link prediction: the power of maximal entropy random walk. In *Proceedings of the 20th ACM International Conference on Information and Knowledge Management*, pages 1147–1156. ACM, 2011.
- [46] Yongjun Li, Zhen Zhang, You Peng, Hongzhi Yin, and Quanqing Xu. Matching user accounts based on user generated content across social networks. *Future Gener. Comput. Syst.*, 83:104–115, 2018.
- [47] Hao Liao, Manuel Sebastian Mariani, Matúš Medo, Yi-Cheng Zhang, and Ming-Yang Zhou. Ranking in evolving complex networks. *Phys. Rep.*, 689:1–54, 2017.
- [48] Hao Liao and An Zeng. Reconstructing propagation networks with temporal similarity. *Sci. Rep.*, 5:11404, 2015.
- [49] David Liben-Nowell and Jon Kleinberg. The link-prediction problem for social networks. *J. Am. Soc. Inform. Sci. Tech.*, 58(7):1019–1031, 2007.
- [50] Linyuan Lü, Liming Pan, Tao Zhou, Yi-Cheng Zhang, and H Eugene Stanley. Toward link predictability of complex networks. *Proc. Natl. Acad. Sci.*, 112(8):2325–2330, 2015.
- [51] Linyuan Lü and Tao Zhou. Link prediction in complex networks: A survey. *Physica A*, 390(6):1150–1170, 2011.
- [52] Neo D. Martinez, John J. Magnuson, Timothy. Kratz, and M. Sierszen. Artifacts or attributes? effects of resolution on the Little Rock Lake food web. *Ecological Monographs*, 61:367–392, 1991.
- [53] Víctor Martínez, Fernando Berzal, and Juan-Carlos Cubero. A survey of link prediction in complex networks. *ACM Comput. Surv.*, 49(4):69, 2017.
- [54] Paolo Massa, Martino Salvetti, and Danilo Tomasoni. Bowling alone and trust decline in social network sites. In *Proc. Int. Conf. Dependable, Autonomic and Secure Computing*, pages 658–663, 2009.
- [55] Julian McAuley and Jure Leskovec. Learning to discover social circles in ego networks. In *Advances in Neural Information Processing Systems*, pages 548–556. 2012.
- [56] Matúš Medo, Manuel S Mariani, An Zeng, and Yi-Cheng Zhang. Identification and impact of discoverers in online social systems. *Sci. Rep.*, 6:34218, 2016.
- [57] James Moody. Peer influence groups: Identifying dense clusters in large networks. *Social Networks*, 23(4):261–283, 2001.

- [58] Alessandro Muscoloni and Carlo Vittorio Cannistraci. Local-ring network automata and the impact of hyperbolic geometry in complex network link-prediction. *arXiv preprint arXiv:1707.09496*, 2017.
- [59] Seth Myers and Jure Leskovec. On the convexity of latent social network inference. In *Advances in Neural Information Processing Systems 23*, pages 1741–1749, 2010.
- [60] Mark E. J. Newman. Finding community structure in networks using the eigenvectors of matrices. *Phys. Rev. E Stat. Nonlin. Soft*, 74(3), 2006.
- [61] Tore Opsahl, Filip Agneessens, and John Skvoretz. Node centrality in weighted networks: Generalizing degree and shortest paths. *Social Networks*, 3(32):245–251, 2010.
- [62] Tore Opsahl and Pietro Panzarasa. Clustering in weighted networks. *Social Networks*, 31(2):155–163, 2009.
- [63] Fragkiskos Papadopoulos, Maksim Kitsak, M Ángeles Serrano, Marián Boguná, and Dmitri Krioukov. Popularity versus similarity in growing networks. *Nature*, 489(7417):537, 2012.
- [64] Romualdo Pastor-Satorras, Claudio Castellano, Piet Van Mieghem, and Alessandro Vespignani. Epidemic processes in complex networks. *Rev. Mod. Phys.*, 87(3):925, 2015.
- [65] Sen Pei, Lev Muchnik, José S Andrade Jr, Zhiming Zheng, and Hernán A Makse. Searching for superspreaders of information in real-world social media. *Sci. Rep.*, 4:5547, 2014.
- [66] Sancheng Peng, Aimin Yang, Lihong Cao, Shui Yu, and Dongqing Xie. Social influence modeling using information theory in mobile social networks. *Inf. Sci.*, 379:146–159, 2017.
- [67] Gerard Salton and Michael J. McGill. *Introduction to Modern Information Retrieval*. McGraw-Hill, Inc., New York, NY, USA, 1986.
- [68] Zhesi Shen, Wen-Xu Wang, Ying Fan, Zengru Di, and Ying-Cheng Lai. Reconstructing propagation networks with natural diversity and identifying hidden sources. *Nat. Commun.*, 5:4323, 2014.
- [69] T.J. Sørensen. *A Method of Establishing Groups of Equal Amplitude in Plant Sociology Based on Similarity of Species Content and Its Application to Analyses of the Vegetation on Danish Commons*. Biologiske skrifter. I kommission hos E. Munksgaard, Argentina, Schleswig, Sun, 1948.
- [70] Michele Starnini, Anna Machens, Ciro Cattuto, Alain Barrat, and Romualdo Pastor-Satorras. Immunization strategies for epidemic processes in time-varying contact networks. *J. Theor. Biol.*, 337:89–100, 2013.
- [71] U. Stelzl, U. Worm, M. Lalowski, C. Haenig, F. H. Brembeck, H. Goehler, M. Stroedicke, M. Zenkner, A. Schoenherr, S. Koeppen, J. Timm, S. Mintzlaff, C. Abraham, N. Bock, S. Kietzmann, A. Goedde, E Toksáz, A. Droege, S. Krobitsch, B. Korn, W. Birchmeier, H. Lehrach, and E. E. Wanker. A human protein–protein interaction network: A resource for annotating the proteome. *Cell*, 122:957–968, 2005.
- [72] Lovro Šubelj and Marko Bajec. Ubiquitousness of link-density and link-pattern communities in real-world networks. *Eur. Phys. J. B Condens. Matter*, 85(1):32, 2012.
- [73] Zhi Sun, Qinke Peng, Jia Lv, and Jing Zhang. A prediction model of post subjects based on information lifecycle in forum. *Inf. Sci.*, 337:59–71, 2016.
- [74] Matic Tribušon and Matevž Lenič. Identifying top football players and springboard clubs from a football player collaboration and club transfer networks. *arXiv preprint arXiv:1602.03664*, 2016.
- [75] Christian Von Mering, Roland Krause, Berend Snel, Michael Cornell, Stephen G Oliver, Stanley Fields, and Peer Bork. Comparative assessment of large-scale data sets of protein–protein interactions. *Nature*, 417(6887):399, 2002.
- [76] Lovro Šubelj and Marko Bajec. Robust network community detection using balanced propagation. *Eur. Phys. J. B*, 81(3):353–362, 2011.
- [77] Jian Wang, Reinhilde Veugelers, and Paula Stephan. Bias against novelty in science: A cautionary tale for users of bibliometric indicators. *Research Policy*, 46(8):1416–1436, 2017.
- [78] Duncan J. Watts and Steven H. Strogatz. Collective dynamics of ‘small-world’ networks. *Nature*, 393(1):440–442, 1998.
- [79] Duncan J Watts and Steven H Strogatz. Collective dynamics of ‘small-world’ networks. *Nature*, 393(6684):440, 1998.
- [80] Peipei Xia, Li Zhang, and Fanzhang Li. Learning similarity with cosine similarity ensemble. *Inf. Sci.*, 307:39–52, 2015.
- [81] Zhi Yu, Can Wang, Jiajun Bu, Xin Wang, Yue Wu, and Chun Chen. Friend recommendation with content spread enhancement in social networks. *Inf. Sci.*, 309:102–118, 2015.

- [82] Wayne Zachary. An information flow model for conflict and fission in small groups. *J. of Anthropological Research*, 33:452–473, 1977.
- [83] An Zeng. Inferring network topology via the propagation process. *J. Stat. Mech. Theory Exp.*, 2013(11):11010, 2013.
- [84] Qian-Ming Zhang, Linyuan Lü, Wen-Qiang Wang, Tao Zhou, et al. Potential theory for directed networks. *PloS one*, 8(2):e55437, 2013.